Measuring Issue Specific Ideal Points from Roll Call Votes

Sooahn Shin*

This version: October 14, 2024

Abstract

Ideal points are widely used to measure the ideology and policy preferences of political actors, ranging from voters and legislators to sovereign states. Yet, an outstanding challenge is to estimate ideal points specific to a single issue area. The conventional approach resorts to subsetting voting data, which results in the loss of valuable information and makes comparisons across issue areas ambiguous. To address this, I introduce IssueIRT, a hierarchical Item Response Theory (IRT) model that uses roll-call votes and user-supplied issue labels to estimate issue-specific axes, each running from left to right positions. This approach first estimates multidimensional ideal points using all available voting data, which are then projected onto issue-specific axes to generate single-dimensional, issue-specific ideal points. Furthermore, I develop a measure of issue similarity to compare the alignment of different issue areas on a unified left-to-right spectrum. I demonstrate that IssueIRT effectively captures issue-specific voting behaviors through simulations and applications studies. Specifically, I show cross-party, regional division over monetary policy in the US House of Representatives during the depression of the 1890s. Finally, I show that polarization in Congress has markedly increased across 32 separate issues from 1979 to 2023. The R package `issueirt` is available for implementing IssueIRT.

Keywords: ideal point estimation, issue-specific ideal point, Congress, sectionalism, polarization

*Ph.D. Candidate, Department of Government and Institute for Quantitative Social Science, Harvard University. Email: sooahnshin@g.harvard.edu. URL: https://sooahnshin.com.

1 Introduction

Ideal point estimation, a widely established measurement strategy in legislative studies, is used for mapping the preferences of political actors (e.g. legislators, justices, and states) into geometric positions in a latent policy space. Tracing back to the foundational work by Poole and Rosenthal (1997), social scientists have applied the method extensively to assess the ideological stances of various political actors, including US legislators (Poole and Rosenthal, 1997; Clinton, Jackman and Rivers, 2004), Supreme Court justices (Bailey and Chang, 2001; Martin and Quinn, 2002), state legislators in the U.S. (Shor and McCarty, 2011), US voters (Bafumi and Herron, 2010), members of the European Parliament (Hix, Noury and Roland, 2006), and the United Nations General Assembly (Voeten, 2000; Bailey, Strezhnev and Voeten, 2017).

Despite significant innovations in application and methodological development, an outstanding challenge remains for applied researchers using ideal point estimation methods: measuring ideal points specific to a *single issue area*. In political science research, many studies focus on a specific issue domain where researchers aim to test their theories, often necessitating the measurement of issue-specific preferences or ideology. For example, Jeong (2018) analyzes the positions of members of Congress on foreign policy, building on the literature that has documented the distinctiveness of these positions from domestic policy stances. Issue-specific ideal points are then utilized as key variables in regression models to test hypotheses related to those specific issue areas. You (2022) measures members' preferences for free trade policy and uses them as the main independent variable in regression models to examine whether lobbyists strategically target politicians with similar preferences, for instance.

Both studies use a subset of roll-call votes specific to foreign and trade policy, respectively, to measure issue-specific ideal points. This seemingly straightforward approach, however, may not be universally applicable given a small number of roll-call votes, and also not directly comparable across issues. In the 117th US House of Representative, for example, among 29 policy areas defined by the Congressional Research Service (CRS, 2022), 12 have 10 or fewer non-unanimous roll-call votes. These includes Taxation (1 vote), Social Welfare (4 votes), Foreign Trade and International Finance (8 votes), Education (9 votes), and Civil Rights and Liberties, Minority Issues (10 votes). In these cases, estimating issue-specific ideal points for all 435 members may suffer from high uncertainty due to the lack of information and may even be unidentifiable. More importantly, these issue-specific ideal points are not comparable across different areas without additional assumptions to map them into a single latent space.

In this paper, I introduce a hierarchical IRT model (`IssueIRT`), building upon classic spatial voting theory and Bayesian Item Response Theory (`BIRT`; Clinton, Jackman and Rivers, 2004), to generate issue-specific ideal points. The key idea is to construct a model that estimates an issue-specific axis within the latent policy space. This axis represents a continuum that extends from left wing to right wing positions on the issue, allowing for the projection of multidimensional ideal points onto this axis to generate single dimensional issue-specific ideal points.

The method incorporates two key innovations. First, the proposed method utilizes data on issue labels of roll-calls, which are available for many legislative bodies (e.g., Comparative Agendas Project by Jones et al., 2023, United Nations General Assembly Voting Data by Voeten, Strezhnev and Bailey, 2009). Using this codebook, one can categorize the roll-calls based on their issue areas. Second, the proposed method extends the two-parameter IRT model by establishing a hierarchical framework for the left-to-right direction of the issue-specific axis. Specifically, it focuses on the item discrimination parameter, which represents the difference between Yea and Nay positions in a roll-call vote, and assumes that this parameter is driven by the left-to-right direction of the issue-specific axis. To model this direction, I employ the von Mises-Fisher distribution (vMF), which is widely used for modeling directional data in multidimensional space.

I demonstrate that the proposed method effectively captures issue-specific voting behaviors through simulation and an application studies of the US House of Representatives. Specifically, as a validation study, I revisit the division over monetary issues during the 1890s, focusing on the rise of Populism and sectional division in the "Battle of the Standards" (Frieden, 2016). It is substantively recognized that during this era, the sectional division over monetary issues diverged from partisan division and emerged as a major cleavage in Congress (Bensel, 2000). I show that the proposed method successfully captures this division over monetary issues using roll-call voting data, thus confirming existing historical narratives on the gold-standard debate.

In the main application study, I use `IssueIRT` to examine varying degrees of polarization across multiple issue areas in contemporary Congress. Polarization, often seen as a widening division into liberal and conservative camps, is increasingly evident within the legislative body of the US. Consequently, there exists a growing interest among political scientists for an in-depth analysis of its extent and content. For example, Layman, Carsey and Horowitz (2006) examine polarization across different issue areas, Hill and Tausanovitch (2015) study the time trends of public polarization using a set of policy, and Bateman, Clinton and Lapinski (2017) demonstrate the inadequacy of existing multidimensional models and subsetting approaches for measuring polarization, arguing that they fail to capture policy changes over time. Additionally, a review article by Iyengar et al. (2019) suggest that exploring the relationship between affective polarization and issue-based ideological polarization among the public and elites is a promising avenue for future research. Together, these works highlight the need for a polarization measure that remains comparable across different issues and over time. `IssueIRT` provides a systematic method to assess and compare polarization across various issue areas by mapping issue axes and issue-specific ideal points into a single latent policy space.

The literature on ideal point estimation methods has steadily grown with advancements in computing power and data collection. These methods now encompass a wide range of data sources, including text data (Slapin and Proksch, 2008; Gerrish and Blei, 2011; Vafa, Naidu and Blei, 2020), survey responses (Tausanovitch and Warshaw, 2013), campaign contributions (Bonica, 2014), and social media data (Barberá, 2015; Bond and Messing, 2015). Alongside this expansion, there have been significant developments in both modeling (Goplerud, 2019; Binding and Stoetzer, 2022) and estimation (Carroll et al., 2013; Imai, Lo and Olmsted, 2016; Peress, 2020).

Building on this literature, the advantages of `IssueIRT`—its ability to compare across issue areas and statistical efficiency—can be demonstrated by comparing it to other existing approaches. First, `IssueIRT` facilitates comparison across different issue areas by mapping issue-specific ideal points within a single latent space. In contrast, subsetting results in different latent spaces for each issue area, hindering such comparisons. Relatedly, Moser, Rodríguez and Lofland (2021) employ multiple latent spaces across groups of votes, such as issue areas, to estimate varying legislative preferences. This modeling choice poses a challenge in comparing ideal points across different issue areas. Hence, the method resorts to estimate "stayers"—legislators who maintain their positions across various issue areas—as anchors.

Additionally, `IssueIRT` utilizes the entire voting dataset, leading to greater statistical efficiency. Unlike the subsetting approach, which uses only a subset of data for estimating issue-specific ideal points, `IssueIRT` maximizes the use of available information. This allows researchers to measure issue-specific ideal points even with a limited number of roll-call votes in the subset.

`IssueIRT` identifies issue axes by using user-supplied codebooks, which are widely available in many substantive domains. This feature sidesteps the identification problem arising from the rotational invariance of the likelihood and the need for constraints in multidimensional ideal point models, which often render the resulting estimated dimensions difficult to interpret. For example, Sohn (2017) addresses the identification problem by sampling multidimensional ideal points and discrimination parameters from the Matrix von Mises-Fisher distribution (MvMF). MvMF, an orthogonal matrix extension of vMF (also discussed in Hoff, 2007, 2009 for factor analysis), ensures estimates in each dimension align along maximum variance directions without redundancy. Like other multidimensional ideal point methods, this requires the researcher to interpret the latent dimensions based on their domain knowledge *ex post*. In contrast, `IssueIRT` estimates issue axes specified *ex ante* by user-supplied issue labels.

This also contrasts with other hierarchical IRT models, such as those involving manual coding or text data, which require more effort in data preparation and face data availability restrictions. For instance, Morucci et al. (2024) propose an IRT model variant that aligns latent dimensions with theoretical concepts. Researchers must manually code relationships between roll-call votes and latent dimensions into four categories (positive, negative, null, and unknown), which are then used as priors on the discrimination parameters. Another strand of studies, such as Gerrish and Blei (2012) and Lauderdale and Clark (2014), estimates issue-specific ideal points using text datasets. Gerrish and Blei (2012) apply labeled latent Dirichlet allocation (LDA) to estimate bill issue proportions and adjust deviations from pooled ideal points, while Lauderdale and Clark (2014) combine LDA with an IRT model. This approach requires a text dataset, which may not be readily available for all legislative bodies and often involves additional preprocessing steps.

The rest of the article is structured as follows: Section 2 introduces two motivating applications. Section 3 proposes an ideal point estimation method that infers the issue-specific axis, onto which legislators' ideal points are projected to measure their issue-specific preferences. This section also explains how this model arises from classic spatial voting theory and formally states the properties of the proposed estimand. In Section 4, a Monte Carlo simulation demonstrates that the proposed method effectively captures issue-specific voting behavior, outperforming a `BIRT` (Clinton, Jackman and Rivers, 2004) model applied to a subset of roll-call votes. Additionally, the method successfully identifies the sectional division—Southern Democrats and Western Populists versus Northeastern representatives—in the 1890s US House, consistent with historical accounts of the monetary issue. Section 5 applies the method to study polarization in recent Congresses across different issue areas over time. The article concludes with remarks and discussion in Section 6.

2 U.S. Congress and Issue Specific Preferences

In this paper, I conduct two application studies on the US House of Representatives. The first case is a validation study, examining whether the proposed method successfully captures divisions over a prominent issue area that deviates from conventional partisan alignment, as explored in existing studies (Bensel, 2000; Frieden, 2016). The second case is the main application study, where I apply the proposed method to explore the dynamics of polarization across different issue areas in contemporary Congress.

2.1 The Rise of Populism and Sectional Division in the 1890s

Political scientists have recognized that there were, throughout the history of the US Congress, numerous moments in which the conventional partisan alignment was not dominant across issue areas. In fact, the cleavage for the key policy areas may have deviated greatly from the conventional partisan alignment. When working with such cases, researchers need to differentiate carefully between distinct issues, to avoid the danger of lumping correlated yet sufficiently distinct issues into a single dimension and treating the remaining variations as obsolete. One prominent example is the politics in the US House of Representatives during the 1890s.

In the 1890s, the congressional and electoral politics in the US revolved around the debate over two alternative monetary standards (silver *versus* gold), commonly referred to as the "Battle of the Standards" (Frieden, 2016 and chapter 6 of Bensel, 2000; for a historical overview, see White, 2017). On one side stood the "Silverites," calling for the free coinage of silver at a sixteen-to-one ratio against gold – which effectively meant the devaluation of the dollar. The aim was to protect agricultural producers, located across the South and the West, from the sharp decline in farm prices and enhance their competitiveness in the world market. On the other side stood the "Goldbugs," whose aim was to stabilize the currency with a fixed exchange rate and to insulate monetary policy from popular control. The "Goldbugs" were mainly from the international financial community of New York City and the big cities in the Northeast.

It is important to note that the division over the monetary standard did not exactly align with the conventional partisan division (Democrat *versus* Republican). Rather, it was a sectional division that pitted the farmers/miners from the South and the West against the international financial community from the Northeast. This was the reason why the Democrats and Republicans exchanged votes in the 1896 Presidential election: the "gold" Democrats of New York City bolted out to support the Republican candidate William McKinley while the "silver" Republicans of the West chose to support the joint Democratic-Populist candidate William Jennings Bryan (Frieden, 2016, p. 118). When it came to monetary policy, partisanship was not the rule.

How can we test this existing narrative with an empirical study? This points to the necessity of a principled way of measuring issue-specific ideal points along with a way to compare different issue areas that provides the applied researchers with a clear picture of underlying political cleavages. In this paper, I use the roll-call votes from the 52nd to 54th US House of Representatives collected by `voteview` (Lewis et al., 2022), and the issue labels from American Institutions Project (Bateman, Katznelson and Lapinski, 2022; Katznelson and Lapinski, 2006) to analyze the division over monetary issue during this period.

2.2 Contemporary Congress and Polarization

"America, we are told, is a divided nation," state Iyengar et al. (2019), referring to the widespread consensus that Democrats and Republicans increasingly disagree on policy issues in Congress. Political polarization is one of the most prolific topics within political science, spurring ongoing efforts to conceptualize and measure the degree of polarization. A notable approach defines polarization as the "separation of politics into liberal and conservative camps" (McCarty, Poole and Rosenthal, 2006, p.3), and uses roll-call voting data to argue that the average ideological positions of Congressional Democrats and Republicans have become increasingly divergent over time.

There has been significant interest among political scientists in conducting in-depth analyses of the extent and content of polarization, particularly in relation to its dynamics across different issue areas. For instance, in its review of party polarization and partisan change, Layman, Carsey and Horowitz (2006) raise a question about the dynamics of polarization across different issue areas: do new partisan conflicts on one issue displace older ones *or* does the partisan conflict extend from older to newer issues? They revisit the concept of 'conflict displacement,' which posits that when a new crosscutting issue dimension emerges, the parties become increasingly polarized on this new issue while converging on the previously dominant line of cleavage. In other words, this view suggests that an intensification of party polarization over racial and cultural issues would coincide with a decline in partisan conflict on social welfare issues. The authors challenge this perspective based on their empirical study using roll-call votes. Instead, they contend that contemporary parties have become increasingly divided on all major issue areas, a process they term 'conflict extension.'

Subsequent studies also highlight the benefits of using a proper measure of polarization within specific issue areas. Hill and Tausanovitch (2015) study the time trends of public polarization by fitting a multinomial IRT model to policy questions from the American National Election Studies and compare them to trends in congressional polarization. As a robustness check for their main estimation of a single-dimensional ideology, they conducted a subsetting analysis focused on social issues. Bateman, Clinton and Lapinski (2017) warn of the inadequacy of existing multidimensional models and subsetting approaches for measuring polarization, particularly when examining political conflicts related to civil rights since 1877. Specifically, they demonstrate that the estimated party medians and roll-call positions from a subsetting analysis of the civil rights dimension deviate from historical expectations, due to the failure to capture changes in policy content. Additionally, Iyengar et al. (2019), in a review article on affective polarization, suggest that exploring the relationship between affective polarization among the public and issue-based ideological polarization among both the public and elites is a promising avenue for future research.

As Lee (2015) pointed out, "[a]ggregating across the wide and changing range of issues facing the federal government to arrive at a single summary measure of ideological polarization raises thorny methodological questions." What a detailed analysis of polarization requires, then, is a measure of polarization for specific issue areas. Particularly, it is essential to use a measure that captures the preferences of Congress members on a specific issue so that researchers can quantify its divergence across parties. More importantly, the method should allow for the comparison of issue-specific preferences across different areas over time. This can be accomplished by mapping these issue-specific ideal points onto a single latent policy space and extending the model to a dynamic one, as proposed in this paper. To analyze varying degrees of polarization across issue areas in the US, I use roll-call votes from the 96th to the 117th US House of Representatives collected by `voteview` (Lewis et al., 2022) and issue labels assigned by legislative analysts at the Congressional Research Service from `congress.gov` (CRS, 2022).

3 Proposed Methodology

In this section, I introduce a hierarchical IRT model, `IssueIRT`, to infer issue-specific axes and propose a method for measuring legislators' issue-specific preferences by projecting their ideal points onto this axis. First, I briefly review spatial voting theory and its geographic explanation to provide intuition behind the `IssueIRT` model. Next, I present the model with an illustration based on an application study, and formally describe the properties of the proposed issue-specific ideal points. Finally, I detail the estimation procedure of the proposed method.

3.1 Setup and Background

Suppose we wish to analyze the voting behavior of n legislators, $i = 1, 2, \ldots, n$, for m roll-call votes, $j = 1, 2, \ldots, m$. As illustrated in Table 1, I use two data sources: roll-call voting data of n legislators on m roll-calls and issue labels for these m roll-calls to analyze legislators' issue-specific preferences. Let $z_j \in \{1, \ldots, k\}$ denote the issue label of the j-th roll-call. In Section 3.6, I provide additional details regarding issue labels, including how the model handles misspecified labels. I adopt the framework of standard multidimensional ideal point estimation, motivated by a spatial voting model based on random utility. The core idea is that each legislator possesses a favorable location, or ideal point, in the policy space. They vote Yea if the utility of voting Yea exceeds that of voting Nay, and vice versa. This utility is jointly determined by the proximity of the proposal suggested in the roll-call to the legislator's ideal point and a random noise.

	Roll-call #1	**Roll-call #2**	**Roll-call #3**	…	**Roll-call #m**
Issue (z_j)	Civil Rights (2)	Defense (7)	Agriculture (10)	…	Defense (7)
Legislator 1	0	0	1	…	0
Legislator 2	1	1	0	…	0
⋮	⋮	⋮	⋮	⋱	⋮
Legislator n	1	0	1	…	1

Table 1: Example of (1) roll-call voting data (second to the last row; $\{y_{ij}\}_{i=1,j-1}^{n,m}$) and (2) issue labels (first row; $\{z_j\}_{j=1}^{m}$).

To formally state this, assume that each legislator i votes Yea on roll-call vote j if the utility of voting Yea (U_{ij}^{y}) is greater than that of voting Nay (U_{ij}^{n}), and vice versa. Let $\boldsymbol{x}_i$ denote a d-dimensional column vector of ideal point of legislator i, where d is the number of dimensions in the latent policy space and $d \geq 2$. Similarly, let $\boldsymbol{o}_j^{\text{y}}$ and $\boldsymbol{o}_j^{\text{n}}$ denote the d-dimensional column vectors of the location of Yea and Nay, respectively, for roll-call j. In the literature, $\boldsymbol{o}_j^{\text{y}}$ and $\boldsymbol{o}_j^{\text{n}}$ are also known as the locations of the "proposal" and "status quo," respectively (Peress, 2013). The Yea utility comprises a deterministic part (u_{ij}^{y}) and a stochastic part (ϵ_{ij}^{y}), where the deterministic part is defined by the distance between the legislator's ideal point and that of the roll-call in the latent policy space. This is similar for the Nay utility. As mentioned above, a legislator is more likely to vote Yea if the proposal's location is closer to their ideal point. Following `BIRT` (Clinton, Jackman and Rivers, 2004), I assume a quadratic utility function with Euclidean distance: $u_{ij}^{\mathrm{y}} := -\|\boldsymbol{x}_i - \boldsymbol{o}_j^{\mathrm{y}}\|^2$, where $\|\cdot\|$ denotes the Euclidean norm. The difference of stochastic utility, $\epsilon_{ij}^{\mathrm{y}} - \epsilon_{ij}^{\mathrm{n}}$, is assumed to be independent and identically distributed random noise, following a standard normal distribution as in `BIRT`. Accordingly,

$$U_{ij}^{\mathrm{y}} = u_{ij}^{\mathrm{y}} + \epsilon_{ij}^{\mathrm{y}} = -\|\boldsymbol{x}_i - \boldsymbol{o}_j^{\mathrm{y}}\|^2 + \epsilon_{ij}^{\mathrm{y}}$$
$$U_{ij}^{\mathrm{n}} = u_{ij}^{\mathrm{n}} + \epsilon_{ij}^{\mathrm{n}} = -\|\boldsymbol{x}_i - \boldsymbol{o}_j^{\mathrm{n}}\|^2 + \epsilon_{ij}^{\mathrm{n}}$$

where $\epsilon_{ij}^{\mathrm{y}} - \epsilon_{ij}^{\mathrm{n}} \sim \mathcal{N}(0,1)$. Let $y_{ij} = 1$ if legislator i vote Yea on roll-call j, and $y_{ij} = 0$ otherwise. It follows that

$$\begin{aligned}
\Pr(y_{ij} = 1) &= \Pr(U_{ij}^{\mathrm{y}} > U_{ij}^{\mathrm{n}}) \\
&= \Pr(u_{ij}^{\mathrm{y}} - u_{ij}^{\mathrm{n}} > \epsilon_{ij}^{\mathrm{n}} - \epsilon_{ij}^{\mathrm{y}}) \\
&= \Pr(\|\boldsymbol{x}_i - \boldsymbol{o}_j^{\mathrm{n}}\|^2 - \|\boldsymbol{x}_i - \boldsymbol{o}_j^{\mathrm{y}}\|^2 > \epsilon_{ij}^{\mathrm{n}} - \epsilon_{ij}^{\mathrm{y}}) \\
&= \Phi\left(\underbrace{\|\boldsymbol{x}_i - \boldsymbol{o}_j^{\mathrm{n}}\|^2}_{\substack{\text{distance between} \\ \text{Nay and ideal point}}} - \underbrace{\|\boldsymbol{x}_i - \boldsymbol{o}_j^{\mathrm{y}}\|^2}_{\substack{\text{distance between} \\ \text{Yea and ideal point}}} \right) \qquad (1) \\
&= \Phi\left(\underbrace{2(\boldsymbol{o}_j^{\mathrm{y}} - \boldsymbol{o}_j^{\mathrm{n}})^\top}_{\substack{\text{discrimination} \\ \text{parameter}}} \boldsymbol{x}_i - \underbrace{(\boldsymbol{o}_j^{\mathrm{y}\top} \boldsymbol{o}_j^{\mathrm{y}} - \boldsymbol{o}_j^{\mathrm{n}\top} \boldsymbol{o}_j^{\mathrm{n}})}_{\substack{\text{difficulty} \\ \text{parameter}}} \right) \qquad (2)
\end{aligned}$$

where $\Phi(\cdot)$ is the cumulative distribution function of the standard normal distribution. Clinton, Jackman and Rivers (2004) connects this model to two-parameter IRT model, where they reparameterize $2(\boldsymbol{o}_j^{\mathrm{y}} - \boldsymbol{o}_j^{\mathrm{n}})$ as β_j, an item discrimination parameter, and $\boldsymbol{o}_j^{\mathrm{y}\top} \boldsymbol{o}_j^{\mathrm{y}} - \boldsymbol{o}_j^{\mathrm{n}\top} \boldsymbol{o}_j^{\mathrm{n}}$ as α_j, an item difficulty parameter.

3.2 Geometric Interpretation

I now explore the geometric implications of the discrimination parameter $2(\boldsymbol{o}_j^{\mathrm{y}} - \boldsymbol{o}_j^{\mathrm{n}})$ as an axis and propose a hierarchical model. To begin, I illustrate the geometric interpretation of the transition from Equation (1) to Equation (2) to elaborate on the idea of the discrimination parameter as an axis. Equation (1) implies that the probability of a Yea vote depends on how much closer the Yea position is to the legislator's ideal point compared to the Nay position. The first key idea is to understand that comparing whether one's ideal point is closer to the Yea or Nay location is equivalent to comparing the projection of one's ideal point onto the line connecting the Yea and Nay locations with the actual locations of Yea and Nay. This concept is illustrated in Figure 1 using a toy example and formally stated in Proposition 1.

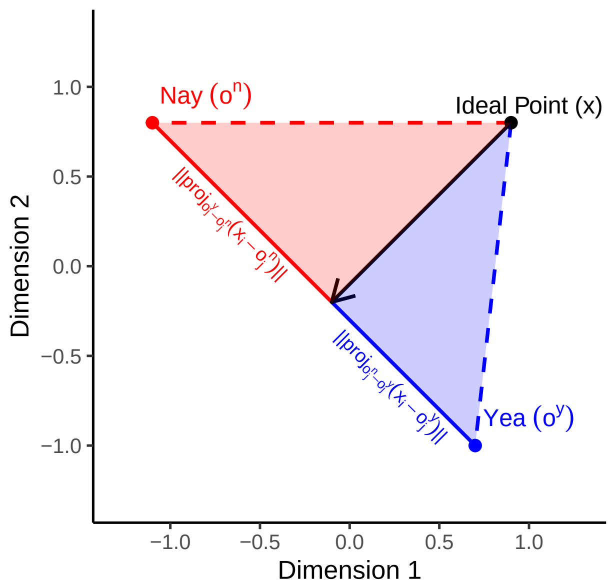

Figure 1: Illustration of spatial voting theory with a toy example in two-dimensional policy space. Here, the black circle denotes the ideal point of a legislator ($\boldsymbol{x}$); the blue circle, the Yea location ($\boldsymbol{o}^{\mathrm{y}}$); and the red circle, the Nay location ($\boldsymbol{o}^{\mathrm{n}}$). The probability of a Yea vote depends on the difference in squared Euclidean distance between the Yea location and the ideal point (blue dashed line) and that between the Nay location and the ideal point (red dashed line). Note that, based on the Pythagorean theorem, the difference in these distances is equivalent to the difference in squared Euclidean distance between the Yea location and the projected ideal point (blue solid line) and that between the Nay location and the projected ideal point (red solid line). Intuitively, this is because the two right-angled triangles, blue on the right and red on the left, share the same altitude (black arrow).

Proposition 1 (Geometry of Spatial Voting Theory)**.** Let $\boldsymbol{x}_i$ be the ideal point of legislator i, $\boldsymbol{o}_j^{\mathrm{y}}$ be the location of Yea, and $\boldsymbol{o}_j^{\mathrm{n}}$ be the location of Nay, where $\boldsymbol{x}_i, \boldsymbol{o}_j^{\mathrm{y}}, \boldsymbol{o}_j^{\mathrm{n}} \in \mathbb{R}^d$ with $d \geq 2$. Then, the probability of Yea on roll-call j is as follows:

$$\Pr(y_{ij} = 1) = \Phi\left(\underbrace{\|\mathrm{proj}_{\boldsymbol{o}_j^{\mathrm{y}} - \boldsymbol{o}_j^{\mathrm{n}}}(\boldsymbol{x}_i - \boldsymbol{o}_j^{\mathrm{n}})\|^2}_{\substack{\text{distance between Nay and}\\ \text{the projected ideal point}}} - \underbrace{\|\mathrm{proj}_{\boldsymbol{o}_j^{\mathrm{n}} - \boldsymbol{o}_j^{\mathrm{y}}}(\boldsymbol{x}_i - \boldsymbol{o}_j^{\mathrm{y}})\|^2}_{\substack{\text{distance between Yea and}\\ \text{the projected ideal point}}} \right)$$

where $\mathrm{proj}_{\boldsymbol{a}}\boldsymbol{b}$ denotes the projection of $\boldsymbol{b}$ onto $\boldsymbol{a}$.

Proposition 1 shows that the probability of a Yea vote depends on the projection of the legislator's ideal point onto the line connecting the locations of Yea and Nay. This implies that the line connecting Yea and Nay acts as an axis along which the legislator's ideal point is projected to measure their preference for the roll-call. That is, if the projection is located left on this axis, they are more likely to vote Nay, and vice versa.

To the best of the author's knowledge, building a hierarchical model based on the direction of the roll-call specific axis is novel in the ideal point estimation literature. However, similar geometric interpretations and conceptualization have been widely accepted in this subject. For instance, the concept of a "cutting line" from Poole and Rosenthal (1997), which separates Yea and Nay votes, is frequently used to interpret the dimensions of latent policy space. This line, orthogonal to the discrimination parameter $2(\boldsymbol{y}_j - \boldsymbol{n}_j)$, passes through the midpoint between the Yea and Nay locations. Therefore, legislators positioned along this line have equal utility for Yea and Nay votes. More importantly, Sohn (2017) similarly conceptualized issue-specific direction by averaging discrimination parameters within the same issue category. Sohn (2017) used this approach to summarize the results of their estimated model which focuses on identifying ideal points with uncorrelated dimensions. In contrast, the main motivation of this paper is the inference of issue-specific ideal points. Therefore, I incorporate a similar concept as a core component of the method, directly parameterizing the direction of the issue-specific axis within the model and utilizing issue labels as inputs to the model.

3.3 IssueIRT Model

Based on this geometric interpretation, I introduce a key assumption of the model: the direction of this roll-call axis is sampled from a distribution centered around the issue-specific axis. To illustrate this, in Remark 1 of the Appendix, I show that the discrimination parameter $2(\boldsymbol{o}_j^{\mathrm{y}} - \boldsymbol{o}_j^{\mathrm{n}})$ can be factored into (1) the Nay-to-Yea direction of such a roll-call specific axis and (2) a scale factor. I then propose a hierarchical model based on (1). Specifically, I assume that the direction of the roll-call-specific axis is drawn from a von Mises-Fisher distribution centered at the direction of the issue-specific axis. This forms the core idea of the proposed model, which is outlined below.

Data generating process. The proposed `IssueIRT` model assumes the following data generating process (DGP):

$$\boldsymbol{u}_j \sim \mathrm{vMF}_d(\boldsymbol{\theta}_{z_j}, \rho), \quad \forall j$$

$$\Pr(y_{ij} = 1) = \Phi(w_j \boldsymbol{u}_j^\top \boldsymbol{x}_i - \alpha_j), \quad \forall i, j$$

where $\text{vMF}(\cdot)$ denotes the probability density function of the von Mises-Fisher distribution, $w_j > 0$, and $\|\boldsymbol{u}_j\| = 1$ for all j. Von Mises-Fisher distribution is a spherical analogue to the Gaussian distribution on the unit sphere. A special case of this when $d = 2$ is von Mises distribution, also known as the circular normal distribution. In this model, votes are coded in a way that Yea votes correspond to a right-leaning position, and vice versa. For further details on the discussion of sign-flip and anchoring, refer to Section 3.6. Here, $\boldsymbol{u}_j$ denotes a unit vector in the direction from left to right on the j roll-call. For ease of understanding, the terms "unit vector" and "direction vector" are used interchangeably. We assume that $\boldsymbol{u}_j$ is sampled from a von Mises-Fisher distribution of which mean lies on $\boldsymbol{\theta}_{z_j}$, a unit vector in the direction from left to right on issue z_j, and concentration parameter is denoted by ρ. Thus, $\boldsymbol{\theta}_{z_j}$ represents the direction of an issue-specific axis in this latent policy space, and ρ determines how much jth roll-call deviates from its issue z_j in terms of left-to-right direction.

The vote choice of the ith legislator on the jth roll-call is jointly determined by three bill parameters – $\boldsymbol{u}_j, w_j$, and α_j – and the ideal point of legislator ($\boldsymbol{x}_i$). Here, w_j denotes a magnitude of the difference between supporting the jth roll-call and opposing it ($w_j > 0$). Observe that $w_j\boldsymbol{u}_j$ corresponds to a discrimination parameter while α_j is a difficulty parameter in the standard two-parameter IRT model. That is, $\boldsymbol{u}_j = (\boldsymbol{o}_j^{\text{y}} - \boldsymbol{o}_j^{\text{n}})/\|(\boldsymbol{o}_j^{\text{y}} - \boldsymbol{o}_j^{\text{n}})\|$ corresponds to a unit vector of the discrimination parameter, where Nay represents a left-leaning vote, and Yea represents a right-leaning vote; $w_j = \|2(\boldsymbol{o}_j^{\text{y}} - \boldsymbol{o}_j^{\text{n}})\|$ is the scale factor of the discrimination parameter; and $\alpha_j = \boldsymbol{o}_j^{\text{y}\top}\boldsymbol{o}_j^{\text{y}} - \boldsymbol{o}_j^{\text{n}\top}\boldsymbol{o}_j^{\text{n}}$ is a standard item difficulty parameter. Hence, the `IssueIRT` model naturally extends the two-parameter IRT model by incorporating a hierarchical structure for issue-specific bill parameters. Figure 2 illustrates the idea with a toy example.

Prior distributions. We choose the prior distributions as follows:

$$\boldsymbol{x}_i \sim \mathcal{N}_d(\mathbf{0}, \mathbb{I}), \quad \alpha_j \sim \mathcal{N}(0, \kappa), \quad w_j \sim \mathcal{TN}(0, \kappa; 0, \infty)$$
$$p(\{\boldsymbol{\theta}_z\}_{z=1}^k, \rho) \propto \left\{ \frac{\rho^{d/2-1}}{\mathrm{I}_{d/2-1}(\rho)} \right\}^a \exp\left(\sum_{z=1}^k b\rho\boldsymbol{\theta}_z^\top \boldsymbol{\theta}_0 \right) \tag{3}$$

where $\mathcal{TN}(\cdot)$ is a truncated normal distribution, I_ν is the modified Bessel function of the first kind of order ν, and $\boldsymbol{\theta}_0$ is the mean of $\boldsymbol{\theta}_z$. Note that Equation (3) is a joint conjugate prior for $\{\boldsymbol{\theta}_z\}_{z=1}^k$ and ρ (Straub, 2017). Here, we set $a = 0.01, b = 0.001$ and $\kappa = 5$ for diffuse priors, and $\boldsymbol{\theta}_0 = \mathbf{0}$. This choice essentially implies that it does not assume any prior knowledge about the issue-specific

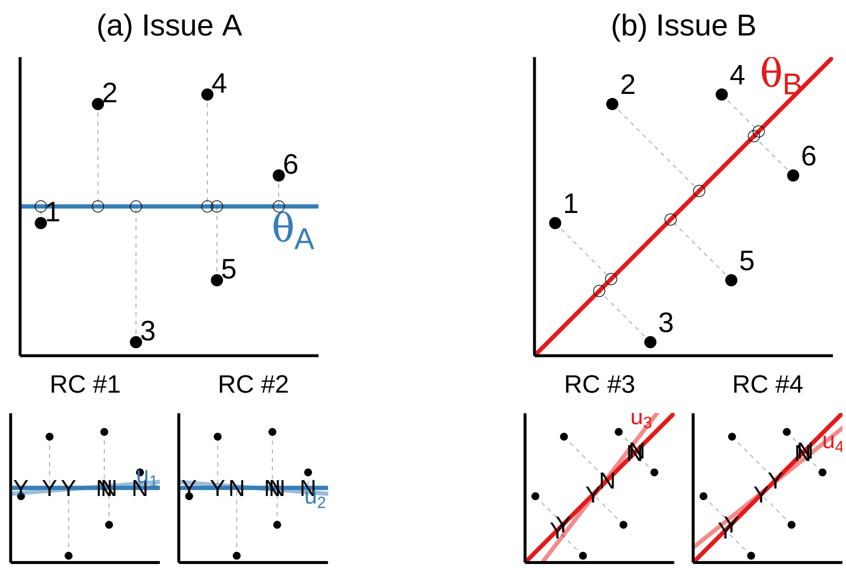

Figure 2: Illustration of the data generating process. Suppose there are 2 issue areas, 6 legislators, and 4 roll-calls. (a) In the top figure, issue A is represented by an axis in the direction of $\boldsymbol{\theta}_A$. Legislators are aligned from 1 (left) to 6 (right) on this axis. In the bottom figures, roll-calls #1 and #2, which belong to issue A, have directions centered at $\boldsymbol{\theta}_A$ (i.e., $\boldsymbol{u}_1$ and $\boldsymbol{u}_2$, respectively). This is reflected in the voting behavior, shown by how Yea and Nay votes are divided. (b) In the top figure, issue B is represented by an axis in the direction of $\boldsymbol{\theta}_B$. Legislators are aligned in the order of 3-1-5-2-6-4 on this axis. In the bottom figures, roll-calls #3 and #4, which belong to issue B, have directions centered at $\boldsymbol{\theta}_B$ (i.e., $\boldsymbol{u}_3$ and $\boldsymbol{u}_4$, respectively).

axis.

Illustration using real data. To facilitate the understanding of the proposed model, I illustrate the substantive interpretation of the DGP using a real example and its estimates from the first application study: the rise of Populism and sectional division in the 1890s.

As mentioned in Section 2.1, a major cleavage in political economy issue during this period evolved around the division over the gold standard: Southern Democrats and the Populists from the West (*anti-gold standard*) v.s. Northeastern representative (*pro-gold standard*). The `IssueIRT` model assumes that within the latent policy space, there exists an axis representing the political economy issue area. Ideal points located to the left of this axis prefer *anti-gold standard* policies, while those to the right prefer *pro-gold standard* policies. In this specific example, I use the terms *pro-gold standard* and *anti-gold standard* instead of "right-wing" and "left-wing" to avoid confusion. The unit vector of this axis is denoted by $\boldsymbol{\theta}_{\text{pe}}$, which is visualized as a dark orange arrow in Figure 3 (a). In other words, Democrats and Populists who are located on the left side of this arrow support *anti-gold standard* policies, while Republicans and other Democrats who are located on the right

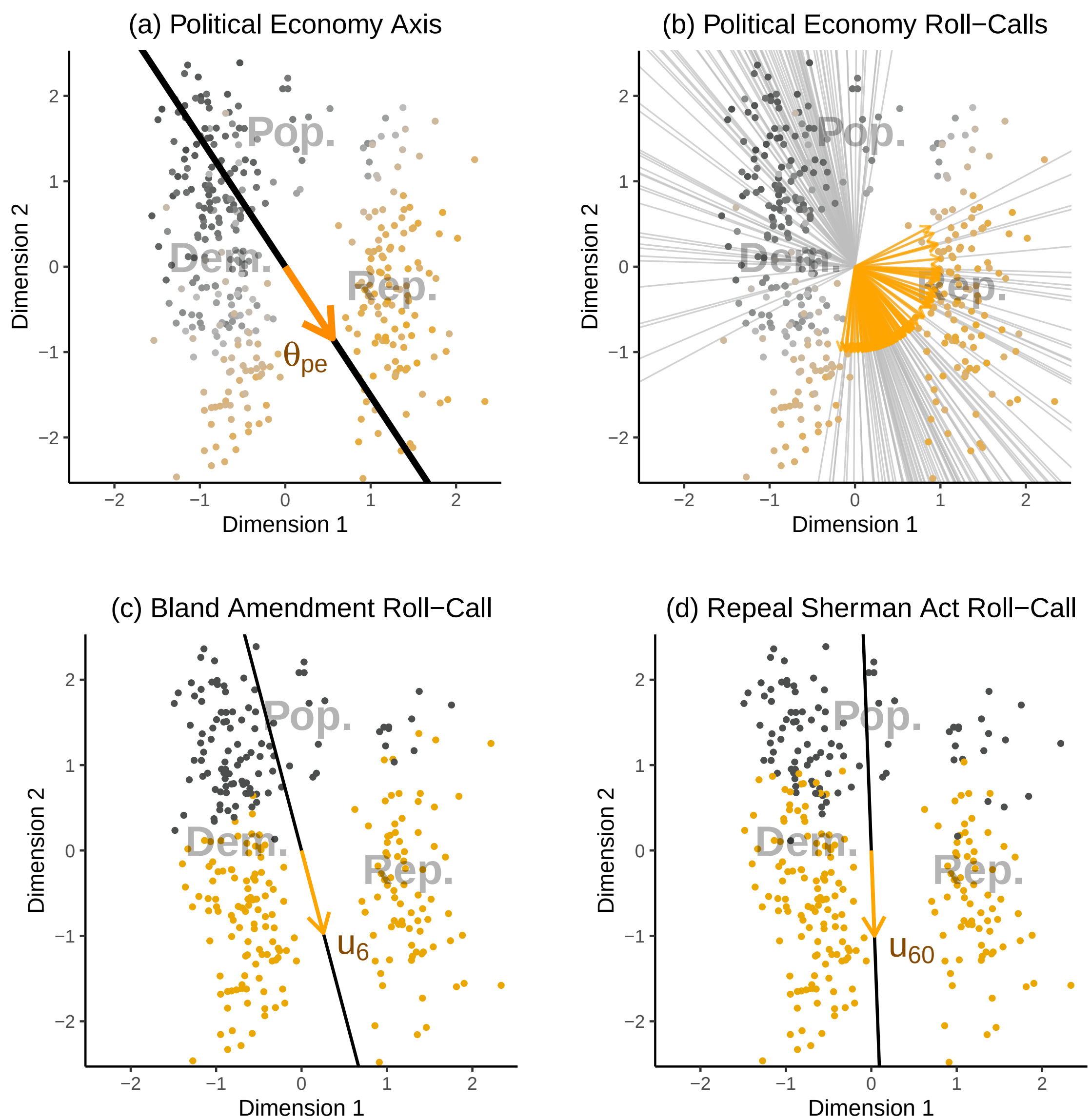

Figure 3: Illustration of the `IssueIRT` model using an application study of the 53rd US House of Representatives (see Section 5 for more details; I use Tier 2 issue labels from Bateman, Katznelson and Lapinski, 2022). In all subfigures, each circle denotes the ideal point of a legislator, and text labels denote party means. For (a) and (b), the color of ideal points is scaled with average votes on political economy roll-calls (silver denotes more frequent *anti-gold* votes, and gold denotes more frequent *pro-gold* votes). For (c) and (d), the color of ideal points indicates a single vote on roll-call #6 on the Bland Amendment and #60 on the Sherman Silver Purchase Act, respectively (silver denotes *anti-gold* votes and gold denotes *pro-gold*. votes). (a) The direction of the political economy issue axis ($\boldsymbol{\theta}_{\text{pe}}$) is visualized as a dark orange arrow. (b) The directions of roll-calls that belong to the political economy are visualized as light orange arrows ($\boldsymbol{u}_z$ where z = pe) which cetered around that of the political economy axis. (c) The direction of roll-call number 6 ($\boldsymbol{u}_6$) is visualized as a light orange arrow. (d) The direction of roll-call number 60 ($\boldsymbol{u}_{60}$) is visualized as a light orange arrow. Across the subfigures, legislators located at the tail of the arrow voted *anti-gold*, while those at the head voted *pro-gold*, as expected from the model.

side of this arrow support *pro-gold standard* policies.

Now, based on the hierarchical model, the preference for political economy issue is translated into the voting behavior on roll-calls related to political economy. The left-to-right direction roll-call specific axes, denoted by $\boldsymbol{u}_j$ such that z_j is political economy, is sampled from a von Mises-Fisher distribution centered at $\boldsymbol{\theta}_{\text{pe}}$. This is visualized as orange arrows in Figure 3 (b). An example is the unit vector of roll-call number 6, which pertains to the Bland Amendment. Proposed by Representative Richard Bland (D-MO) during the special session of the 53rd U.S. House of Representatives in August 1893, the amendment aimed at effectively overturning the *pro-gold* intent of a bill that would repeal the Sherman Silver Purchase Act of 1890, by introducing free coinage. In Figure 3 (c), Democrats and Populists located on the left side of the orange arrow voted *anti-gold*, while Republicans and other Democrats on the right side voted *pro-gold*. A similar pattern can be observed in other political economy-related roll-calls, such as roll-call number 60 on the repealing of the Sherman Silver Purchase Act, as shown in Figure 3 (d).

Extension to a dynamic model. Following Martin and Quinn (2002), the `IssueIRT` model can be extended to a dynamic model by incorporating a random-walk model for the ideal points. This can be achieved by adding the following prior to the model:

$$\boldsymbol{x}_{i,t} \mid \boldsymbol{x}_{i,t-1} \sim \mathcal{N}_d(\boldsymbol{x}_{i,t-1}, \Delta), \quad \forall i, t = \underline{T}_i + 1, \ldots, \overline{T}_i$$

where $\underline{T}i$ is the first term legislator i served, and $\overline{T}i$ is the last term legislator i served. In our application, we set the hyperparameter $\Delta = 0.01 \cdot \mathbb{I}$. For the initial time period, we assume that:

$$\boldsymbol{x}_{i,\underline{T}_i} \sim \mathcal{N}_d(\mathbf{0}, \mathbb{I}), \quad \forall i.$$

In words, this implies that the ideal point of a legislator at time t is determined by their previous ideal point at time $t-1$, with a small stochastic noise. As emphasized by Martin and Quinn (2002), this strikes a balance between the strong assumption of fixed ideal points across time and the assumption of independence from the previous time. We do not assume a specific structure for the mean direction of each issue area and treat them as separate issues, thus allowing for divergence over time.

3.4 Issue-Specific Ideal Points

Building upon the `IssueIRT` model, I propose a method for measuring legislators' issue-specific preferences: a projection of their multidimensional ideal point onto the issue-specific axis. Definition 3.1 formally states this quantity.

Definition 3.1 (Issue-Specific Ideal Points)**.** The issue-specific ideal point of legislator i on issue z is defined as follows:

$$x_i^*(z) \equiv \boldsymbol{\theta}_z^\top \boldsymbol{x}_i$$

which is the scalar projection of multidimensional ideal point ($\boldsymbol{x}_i$) onto the issue specific direction ($\boldsymbol{\theta}_z$).

By fitting the `IssueIRT` model, we can estimate the left-to-right direction of each issue area ($\boldsymbol{\theta}_z$). According to earlier-described spatial voting theory, the probability of a Yea vote depends on the projection of the legislator's ideal point onto the line connecting Yea and Nay locations. Analogously, the projection of legislator i's ideal point onto the issue specific axis yields a nice summary of their issue specific preference. Property 1 formally states this property.

Property 1 (Issue-Specific Voting Behavior)**.** Suppose the DGP of the `IssueIRT` model holds. Let $y_{ij}^* \equiv w_j \boldsymbol{\theta}_z^\top (x_i^*(z)\boldsymbol{\theta}_z) - \alpha_j$ such that $z_j = z$. This involves first computing the issue-specific ideal point (x_i^*), projecting it onto the issue-specific axis ($\boldsymbol{\theta}_z$), and calculating the probability of a Yea vote on roll-call j from issue z. Then, the following holds:

$$y_{ij}^* = \mathbb{E}_{\boldsymbol{u}_j}[\mathbf{1}\{y_{ij} = 1\} \mid \boldsymbol{\theta}_z, w_j, \boldsymbol{x}_i, \alpha_j].$$

That is, y_{ij}^* represents the expected vote choice on issue z, with the expectation taken over the random deviation of roll-call j from issue z.

Property 1 shows that if we plug the proposed issue-specific ideal point into the DGP, it can be used to impute legislator i's expected preference on issue z, thereby demonstrating its usefulness as a measure of issue-specific ideology.

Another important property of the issue-specific ideal point is its invariance to rotation of the latent policy space. Intuitively, as the latent space rotates, both the issue-specific direction vectors and the multidimensional ideal points rotate by the same amount, maintaining the same projection and thus yielding equivalent issue-specific ideal points. Therefore, unlike the coordinates themselves $(x_{i1}, \ldots, x_{id})$, the rotation of the policy space does not change the substantive results of these projected ideal points. This is formally stated below.

Property 2 (Invariance to Rotation)**.** For any rotation matrix $\boldsymbol{R}$, i.e. an orthogonal matrix with a determinant of 1,

$$x_i^*(z) \equiv \boldsymbol{\theta}_z^\top \boldsymbol{x}_i = (\boldsymbol{R}\boldsymbol{\theta}_z)^\top \boldsymbol{R}\boldsymbol{x}_i$$

where the right-hand side is issue-specific ideal point under the rotated latent space.

Issue similarity. Issue-specific ideal points not only provide researchers with a concise summary of voting behavior but also offer a similarity measure of different issue areas. Since issue-specific direction vectors lie in the same latent policy space, we can use cosine similarity to measure the similarity between these vectors: $|\cos(\boldsymbol{\theta}_{\text{Issue A}}, \boldsymbol{\theta}_{\text{Issue B}})|$ which ranges from 0 (dissimilar) to 1 (similar). This can be interpreted as the measure of "constraint", the degree to which policy attitudes on one issue aligns with those on the other issue, discussed in Marble and Tyler (2021). A similar measure, `item2vec`, analogous to `word2vec` in text analysis, was introduced by Sohn (2017) and is computed by averaging the cosine similarity between a discrimination parameter of interest and a set of difficulty parameters for comparison.

3.5 Identification

It is well known that two-parameter IRT models are not identified without further restrictions. The additive and scale invariance of the model (i.e., $\boldsymbol{x}_i \to \boldsymbol{x}_i + \boldsymbol{c}$ and $\boldsymbol{x}_i \to \boldsymbol{c}^\top \boldsymbol{x}_i$ for $c \in \mathbb{R}^d$) is not a concern in the proposed model with a normal prior over multidimensional ideal points (Jackman, 2001). However, the rotational invariance of the model (i.e., $\boldsymbol{x}_i \to \boldsymbol{R}\boldsymbol{x}_i$ for a rotation matrix $\boldsymbol{R}$) remains as an issue. As described in Property 2, since both the issue-specific direction vectors and the multidimensional ideal points are rotated by the same amount, the issue-specific ideal points are invariant to these rotations as they are projections of the former onto the latter. Nevertheless, if the multidimensional ideal points are of interest, rotational invariance needs to be addressed. In this regard, we follow Clinton, Jackman and Rivers (2004), which implements one of the identification restrictions discussed in Rivers (2003): placing $d(d+1)$ linearly independent restrictions on the ideal points $\boldsymbol{x}_i$ for $i = 1, \ldots, n$ (also known as Kennedy-Helms restriction). In practice, we fix $d+1$ number of legislators for each iteration of samples (e.g. 3 legislators for $d = 2$).

Another issue in the `IssueIRT` model concerns the sign of the issue-specific unit vectors. Recall that $\boldsymbol{u}_j = (\boldsymbol{y}_j - \boldsymbol{n}_j)/\|(\boldsymbol{y}_j - \boldsymbol{n}_j)\|$ corresponds to a unit vector of the discrimination parameter, which can be interpreted as the direction from Nay to Yea. Here, a Yea vote can represent either a preference of left- or right-wing, depending on the roll-call. In other words, the direction from Nay to Yea on the axis can be flipped depending on the specific context: it may correspond to either a left-to-right or right-to-left direction. Since the DGP of the model assumes that the mean of $\boldsymbol{u}_j$ is centered around a single issue-specific direction (e.g., whose angle is $\pi/2$) rather than a pair of directions (e.g., $\pi/2$ and $-\pi/2$), this sign-flip should be addressed. This can be easily implemented by anchoring a liberal legislator's votes (or the majority of the liberal party's votes) so that Nay votes indicate the vote of this liberal legislator. Similarly, one may use the party of the bill's sponsor. Another solution is to use the posterior mean of the sign of the discrimination parameter as fitted with `BIRT`; if the sign is negative, we flip the Yea and Nay votes, for example. Alternatively, we can use the Bingham distribution instead of the von Mises-Fisher distribution to address the problem using the model. In this context, the Bingham distribution can be understood as a symmetric version of the von Mises-Fisher distribution, allowing us to sample in either the left-to-right or right-to-left direction. As a result, we only need to fix the sign-flip of multidimensional ideal points once, without needing to anchor left votes for each roll-call.

3.6 Estimation

The proposed method for estimating issue-specific ideal points is implemented in two steps. First, we fit the `IssueIRT` model using Markov chain Monte Carlo (MCMC) methods. Specifically, we implement Hamiltonian Monte Carlo (HMC) using Stan (Stan Development Team, 2024) to sample from the posterior distribution of the model parameters. Second, we project the estimated multidimensional ideal points onto the issue-specific axis. An open source `R` package, `issueipe`, is available upon request. Below, I provide some details of the implementation of the method.

Issue label. In the `IssueIRT` model, it is assumed that each roll-call can be categorized into a single issue area. When multiple issue labels are assigned to a roll-call, a new combined issue category can be created. For instance, a roll-call labeled as both "Civil Rights" and "Labor/Employment" could be reclassified under a new category, "Civil Rights/Labor/Employment". Similarly, roll-calls without assigned labels can be categorized solely under "Other", depending on the research question. Unlike the subsetting approach, the proposed method allows for visual inspection of issue-specific direction vectors to identify and correct labeling errors and reassess the model if necessary. Specifically, one may visualize direction vectors as shown in Figure 3 (b) and check for any outliers. Additionally, if two differently labeled roll-calls address the same issue, their estimated direction vectors would appear similar. Section 4 demonstrates the robustness of the proposed method to such issue label misspecification.

Dimensionality. In the proposed method, a potential limitation is the requirement for researchers to specify the dimensionality of the latent policy space, which must exceed two dimensions. This challenge is common in ideal point estimation literature. Typically, the dimensionality of the latent policy space is assumed to be either one or two in various applications. A standard approach is to perform a Scree test, plotting metrics such as eigenvalues to identify the "elbow" in the plot (Poole et al., 2011). It is advisable to conduct a similar test or apply other multidimensional ideal point estimation methods to ascertain the dimensionality of the latent policy space (Sohn, 2017; McAlister, 2021). Importantly, the issue-specific ideal points remain one-dimensional, regardless of the dimensionality of the latent policy space.

Starting values. The proposed method necessitates starting values for the MCMC sampler. For the issue-specific direction vectors, I use the average direction of discrimination parameters, computed by averaging over issue categories, as fitted with the `BIRT` model, to serve as starting values. For the other parameters, I use the posterior mean derived from the `BIRT` model as the initial values. I adopt this approach because, with a sufficient number of roll-calls and issue categories, initialization with random values may result in underflow of the likelihood in Stan. Alternatively, one could use the eigenvalues of the correlation matrix from the roll-call matrix, as is the default in the `ideal` function from Jackman (2020).

Multimodality. A key challenge in sampling a parameter from the von Mises-Fisher distribution is the potential for multimodality. Consider, for instance, a two-dimensional latent policy space. In this scenario, roll-call specific direction vectors are sampled from the von Mises distribution, which spans an angular range of $[-\pi, \pi]$. If the distribution is not sufficiently concentrated away from disconnected regions, such as around π and $-\pi$, sampling within the $[-\pi, \pi]$ range may result in multimodality. This can manifest as one mode near the lower bound and another near the upper bound, leading to the risk of the sampler getting "stuck" in one mode. To mitigate this, I adopt the approach suggested by Pourzanjani et al. (2021) and introduce an independent auxiliary parameter ($r_j \sim \mathcal{N}(1, 0.1)$) for each angle parameter ($\cos(\boldsymbol{u}_j)$). This approach involves transforming the density for sampling over Cartesian coordinates (x_j and y_j), with $x_j = r_j \cos(\boldsymbol{u}_j)$ and $y_j = r_j \sin(\boldsymbol{u}_j)$, to enhance mixing. The same technique is applied for sampling $\boldsymbol{\theta}_z$.

4 Validation Studies

In this section, I conduct Monte Carlo simulations and apply the method to the 1890s US House of Representatives as validation studies.

4.1 Monte Carlo Simulations

To examine the performance of issue-specific ideal points generated from the `IssueIRT` model, I conduct a Monte Carlo simulation. I compare the results with a subsetting approach where we fit a `BIRT` model with a subset of roll-call voting data that consists of single issue area. We assume a two-dimensional policy space where 100 legislators cast their votes on 150 roll-calls across twelve randomly-assigned issue areas ($d = 2$, $n = 100$, $m = 150$, $k = 12$). I use $\{0 \cdot \pi, 1/12 \cdot \pi, 2/12 \cdot \pi, \ldots, 11/12 \cdot \pi\}$ as twelve different issue-specific mean directions, i.e. $\boldsymbol{\theta}_1 = (1, 0)$, $\boldsymbol{\theta}_2 = (0.97, 0.26), \ldots, \boldsymbol{\theta}_{12} = (-0.97, 0.26)$. See Figure 14 in Appendix for an illustration. Once I randomly sample ideal points and bill parameters, I compute each legislator's probability of voting Yea for each roll-call. Note that both `IssueIRT` and `BIRT` models are consistent with this DGP. Then, I apply inverse transform sampling to generate synthetic roll-call votes. All samples are obtained from two chains of $2,000$ MCMC iterations with $1,000$ burn-in trials. I project posterior mean of multidimensional ideal points onto each issue-specific axis to estimate issue-specific ideal points. For the comparison with a subsetting approach, I fit one-dimensional `BIRT` model using the R package `pscl` for each subset of roll-call votes that consists of the same issue area.

Figure 4 presents the results for a subset of issue areas. Each column displays the issue-specific ideal points for four different issue areas. The top figure compares the true ideal points with the estimates using `IssueIRT`, while the bottom figure compares them with the estimates using `BIRT` for the subset of roll-call votes. The results demonstrate that our proposed method successfully recovers issue-specific ideal points, whereas the estimates from the subsetting approach are generally crude. The measurement error of the subsetting approach arises from the small number of roll-calls in each issue area. For example, in issue 1, the subsetting approach uses only 12 roll-calls from this issue area, whereas `IssueIRT` uses the entire voting data for the estimation. This results in similar values of `BIRT` estimates despite differences, as shown by dots aligned horizontally in the

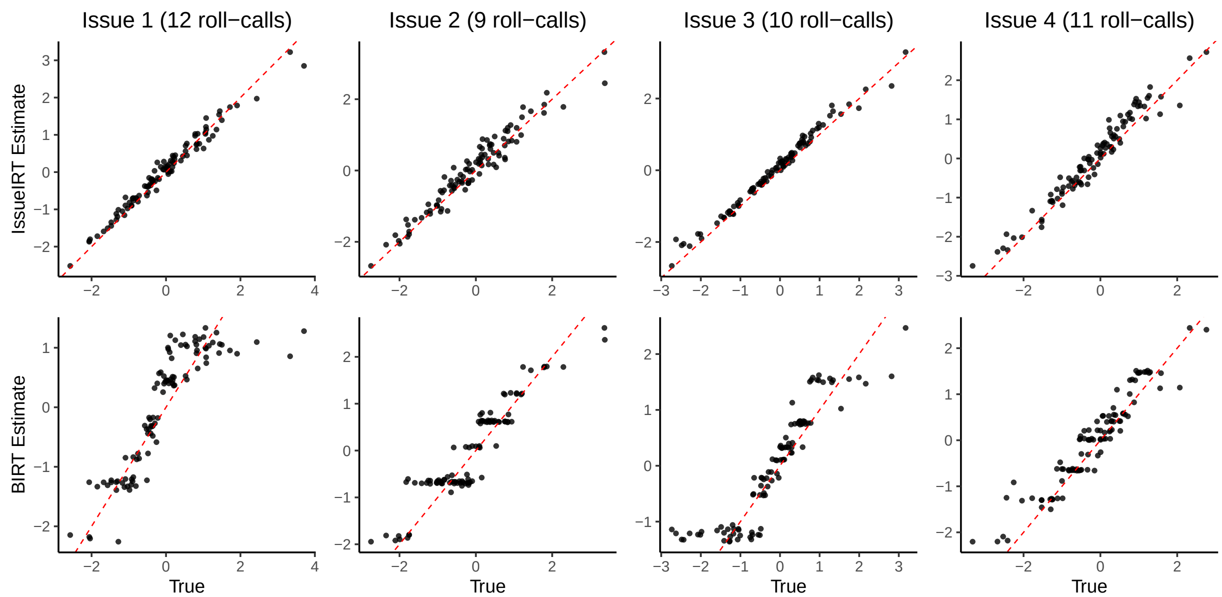

Figure 4: Results of a simulation study with Scenario 1 (correctly specified issue codes). Each column shows the issue-specific ideal points for four of the twelve issue areas. The figure at the top compares true ideal points (x-axis) with the estimates of issue-specific ideal points using `IssueIRT` (y-axis), and the figure at the bottom compares these with the estimates using `BIRT` for the subset of roll-call votes (y-axis). Ideal points aligned with the red dashed diagonal line indicate that the estimates are close to the true values. The results are consistent for the remaining eight issue areas (see Figure 15).

bottom left figure.

This demonstrates that the subsetting approach suffers from loss of information and greater uncertainty in estimation due to the small dataset size, whereas the proposed method fully utilizes all the information available in the entire roll-call voting data. Moreover, unlike the subsetting approach, the proposed method allows for direct comparison of ideal points across different issue areas, as they are mapped in a common latent space. In Appendix D, I show that the same conclusion holds for the case with misspecified issue codes, where we consider a hypothetical scenario in which the researcher mistakenly uses a more granular issue categorization.

4.2 The Rise of Populism and Sectional Division in the 1890s

As discussed in Section 2.1, the congressional and electoral politics during the 1890s United States were largely shaped by the battle between the gold and silver standards. The division over gold aligned with a sectional division rather than a partisan division, forming diverging preferences across different issue areas. I use the roll-call votes from the 52nd (1891-93) to 54th (1895-97) US House of Representatives collected by `voteview` (Lewis et al., 2022), and the issue labels from

American Institutions Project (Bateman, Katznelson and Lapinski, 2022; Katznelson and Lapinski, 2006). The roll-call voting data consists of 337, 372, and 362 representatives with 295, 336, and 161 non-unanimous roll calls for each Congress respectively. I fit `IssueIRT` model and compute the issue-specific ideal points using the estimates of parameters. All samples are obtained from two chains of $50,000$ MCMC iterations with $30,000$ burn-in trials.

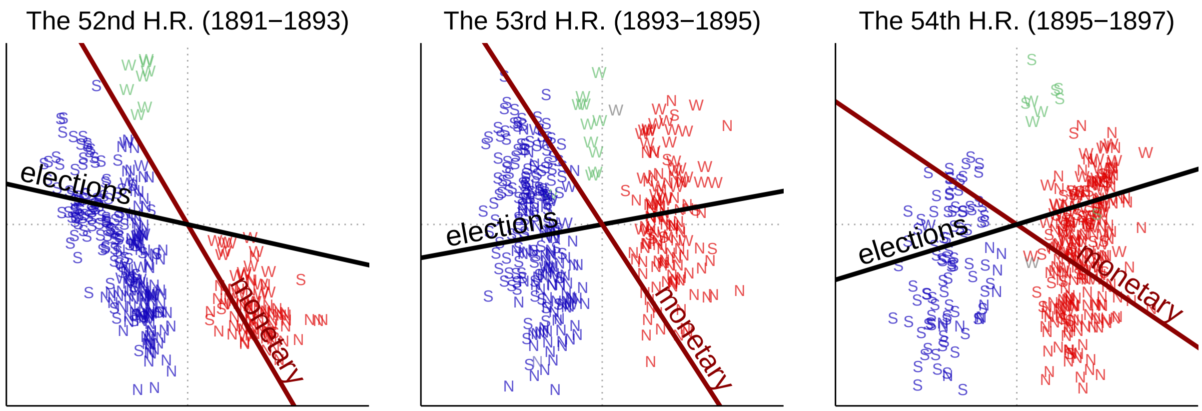

Figure 5: Multidimensional ideal points estimated with the `IssueIRT` model for each of the 52nd, 53rd, and 54th US House of Representatives (left, middle, and right figures, respectively). Each letter at a legislator's ideal point denotes the legislator's section ('N' for Northeastern, 'S' for Southern, and 'W' for Western states), and the color of the letter indicates party affiliation (blue for Democrat, red for Republican, and green for Populist). The black line represents the election-specific axis, and the red line represents the monetary policy-specific axis.

Figure 5 shows the result of multidimensional ideal points with two issue-specific axes, elections and monetary, for each Congress. The roll-calls classified as elections concern contested elections, rules for elections, and campaign finance. Naturally, the legislators' alignment on the election issue represents the partisan alignment. Monetary roll-calls include bills concerning gold and silver standards, the value of the dollar, bond sales (including war bonds), legislation to repay and refund the public debt, and monetary aggregates (Bateman, Katznelson and Lapinski, 2022). Here, we are interested in capturing how preferences toward monetary policy evolve around partisan *versus* non-partisan alignments. We can observe that the alignment on the monetary issue deviates from the partisan alignment in the 52nd, 53rd, and 54th House of Representatives. This is confirmed by the difference between the election-specific axis (black line) and the monetary-specific axis (red line) in terms of their orientation in the policy space. Additionally, the difference between the two axes aligns with the historical trajectory of the Battle of the Standards: from "the beginning of what became a party-rending struggle" over the gold standard during the 52nd H.R. (Bensel, 2000, p.404), to the climax during the 53rd H.R. involving the prompt repeal of the Sherman Act and the proposal of silver seigniorage, and eventually to a standstill in the 54th H.R. following the crushing defeat of the Democrats outside the South in the 1894 midterm elections.

Figure 6: Distribution of sections (top) and party labels (bottom) over monetary issue-specific ideal points for each of the 52nd, 53rd, and 54th US House of Representatives (left, middle, and right figures, respectively). In the top three plots, the orange distribution represents the monetary issue-specific ideal points of Northeastern representatives, the blue distribution represents those of Southern representatives, and the yellow distribution represents those of Western representatives. In the bottom three plots, the blue distribution represents the monetary issue-specific ideal points of Democrats, the green distribution represents those of Populists, and the red distribution represents those of Republicans. Each distribution represents a probability density function estimated with issue-specific ideal points measured by the proposed method.

To further understand the cleavage over monetary issues, we examine how monetary-specific ideal points are distributed by section *versus* party in Figure 6. The top three plots show the density distributions of monetary specific ideal points for Northeastern, Southern, and Western representatives during the 52nd, 53rd, and 54th H.R; the bottom three plots show those of Democrats, Populists, and Republicans. Following Bensel (2000), Southern states include all those that seceded into the Confederacy plus Kentucky, Missouri, Oklahoma, and West Virginia; Western states include all states west of Illinois and Wisconsin not included in the South; the Northeastern states include all the remaining states. In the top three plots, we observe that most of Southern representatives (blue area) have negative monetary ideal points, whereas Northeastern representatives (orange area) have positive monetary ideal points. This aligns with existing studies emphasizing sectional divisions based on contrasting interests over monetary policy: farmers from the South versus the international financial community from the Northeast. Indeed, in the 1896 presidential election, which mainly centered on the monetary question, William Jennings Bryan, the joint Democratic-Populist candidate who opposed the gold standard, lost the support of the gold Democrats, whereas William McKinley, the Republican candidate who opposed the silver standard, lost the support of silver Republicans (Frieden, 2016, p. 118). The bottom three plots confirm this sectional division, showing that the monetary ideal points of Democrats (blue area) were widely dispersed until the 1894 midterm elections when almost 90% of Democrats and Populists represented the South.

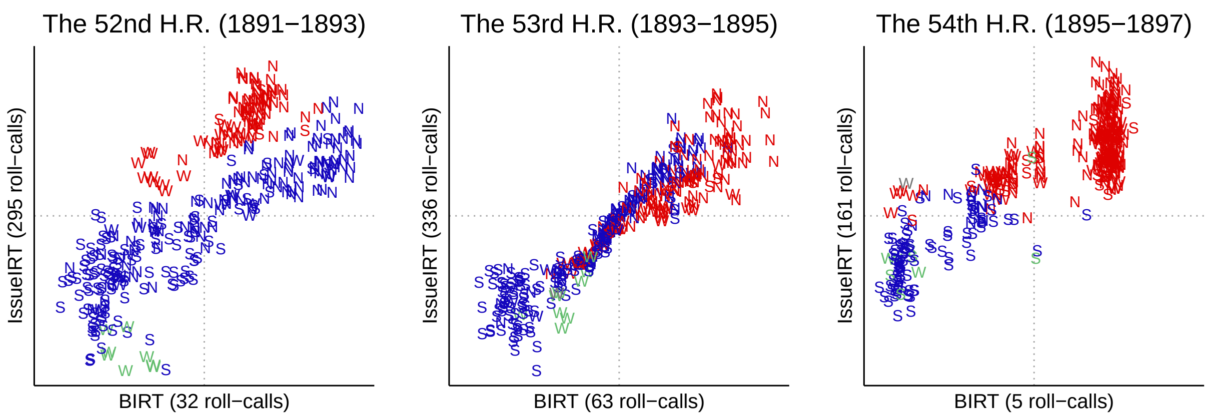

Figure 7: Comparison of monetary policy-specific ideal points measured with `IssueIRT` vs. `BIRT` with subsets for each of the 52nd, 53rd, and 54th US H.R. (left, middle, and right figures, respectively). In each figure, the x-axis represents the estimates of one-dimensional `BIRT`, and the y-axis represents issue-specific ideal points of `IssueIRT`. Each letter denotes the legislator's section ("N" for Northeastern,"" S" for Southern, and "W" for Western states), and the color of the letter indicates party affiliation (blue for Democrats, red for Republicans, and green for Populists). Ideal points aligned with the diagonal line indicate that the estimates are similar in value.

The presented results of issue-specific ideal points cannot be fully captured by a subsetting approach, where we fit the `BIRT` model for each issue-specific subset. In Figure 7, we compare monetary-specific ideal points with one-dimensional `BIRT` estimates using only monetary roll-call votes. We observe that Southern Democrats (blue "S") and Populists (green "W"), who together formed an anti-gold alliance, are positioned at one extreme for both measures. However, due to the small subset of monetary-related roll-calls during the 54th H.R. (5 roll-calls), `BIRT` estimates cannot distinguish Goldbugs among Republicans. The `BIRT` estimates of Republicans in the second quadrant are aligned in a single column, indicating that they share the same value of monetary ideal points despite their nuanced differences. This highlights one of the shortcomings of the subsetting approach, namely the loss of information, as further demonstrated by the density distribution in Figure 25 from Appendix E.1.

5 Application Study: Contemporary Congress and Polarization

Motivated by recent literature on the increasingly intensifying polarization in contemporary Congress as discussed in Section 2.2, I assess the varying degrees of polarization across different issue areas by measuring the distance between party means of the issue-specific ideal points. I use the roll-call votes from the 96th (1979-81) to 117th (2021-23) US House of Representatives collected by `voteview` (Lewis et al., 2022), and the issue labels from `congress.gov` assigned by legislative analysis in the Congressional Research Service (CRS, 2022). According to their documentation, "[t]he term chosen is the one that best describes the focus or predominant subject matter of each measure. Such factors as the congressional committee of referral and the statutory schemes involved may also play a role in the assignment decision." I fit `IssueIRT` model and estimate the issue-specific direction vectors for 32 issue areas.

We use the most widely-used measure of polarization, the distance between party means, based on the issue-specific ideal points. In this study, I conduct two sets of analyses: one examining long-term trends in voting behavior over approximately 40 years, and the other providing a more in-depth analysis of the 1990s. In the first analysis, I measure issue-specific ideal points for each Congress and standardize them to have a mean of zero and a standard deviation of one. Based on these standardized issue-specific ideal points, I compute the absolute difference in party means and report the trend across issue areas.

Figure 8 shows the different levels of polarization across issue areas for each Congress. It illustrates that parties in contemporary US politics have become increasingly divided on all major issue areas. The smoothed line (red curve) has an upward slope, indicating that the polarization level across issue areas has increased over time. Notably, the Congresses following the midterm year of 1994, the 104th to the 106th, mark the point when polarization across issue areas intensified. This is the period when Representative Newt Gingrich (R-GA) ascended to power within the Republican Party with his confrontational style and eventually assumed the Speakership. Indeed in Figure 8, the red diamonds, representing the average across issue areas for each Congress during this period, indicate a sharp increase in polarization levels after the midterm year. The results are robust to other measurements of polarization, such as using the party median instead of the

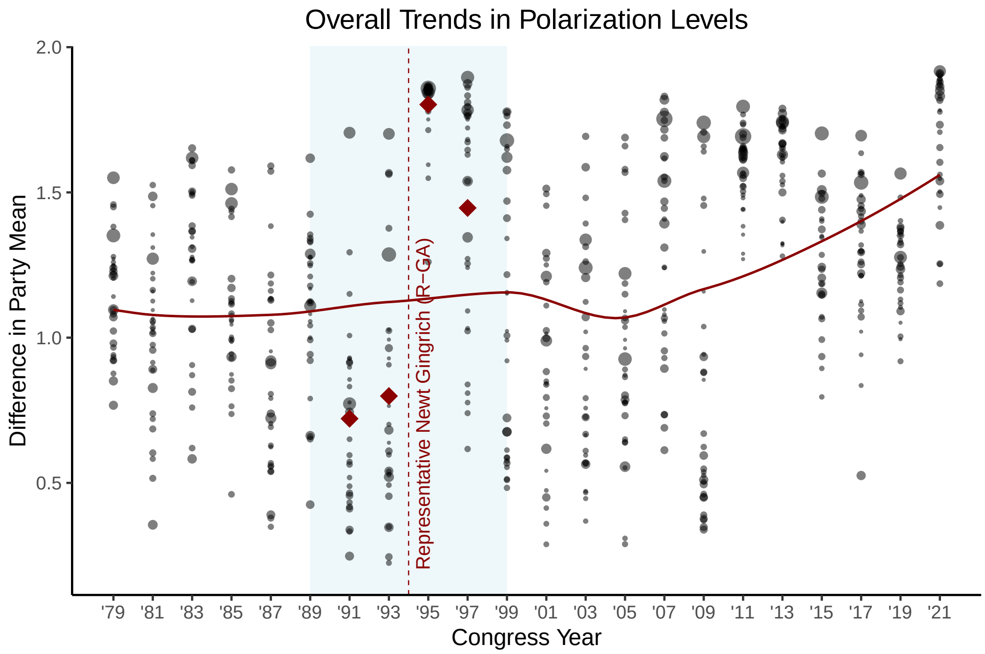

Figure 8: Difference in party means of issue-specific ideal points across the 96th to 117th US House of Representatives. Each point represents an issue area, with the x-axis indicating the Congress year and the y-axis representing the posterior mean of the difference in party means. The size of the point is proportional to the number of roll-calls in each issue area. To measure this difference, I first fit the `IssueIRT` model for each Congress, compute issue-specific ideal points within each Congress, standardize them to have a mean of zero and a standard deviation of 1, and then compute the absolute difference in party means (i.e., the absolute difference between Democrat and Republican parties). The red curve represents a locally weighted scatterplot smoothing curve of the difference in party means over time. The diamond points represent the mean difference across issue areas from the 102nd to the 105th Congress to illustrate the general trend during the 1990s.

mean, and another method of standardizing the issue-specific ideal points to make them robust to outliers (subtracting the median and dividing by the interquartile range). See Appendix E.2 for these results, along with a measurement based on cosine similarity.

To rigorously examine the changes in issue-specific polarization levels over time, we fit a dynamic model to the data. Specifically, we focus on the 101st to 106th House of Representatives, covering the Bush and Clinton presidencies (1989-2000). By using estimates from a dynamic model, one can directly compare the differences in means of issue-specific ideal points without the need for standardization. Furthermore, we can compare how the issue axes evolve over time by mapping them into a single latent policy space using a dynamic model, as we will show for the trade and finance issues later in this section.

Figure 9 provides a summary of polarization across selected issue areas. Notably, issues with initially low polarization levels, "Finance and Financial Sector" and "Economics and Public Finance," had become the most polarized by the end of the Clinton presidency. In contrast, changes in polarization for 3 policy domains – "International Affairs," "Crime and Law Enforcement," and "Armed Forces and National Security" – were relatively modest. We also observe a decrease in polarization for "Foreign Trade and International Finance" and "Transporation and Public Works." The resultant picture of the decade is more nuanced than conventionally understood: rather than a uniform shift across all issues, polarization was an uneven process progressing at divergent speeds and magnitudes depending on the policy substance.

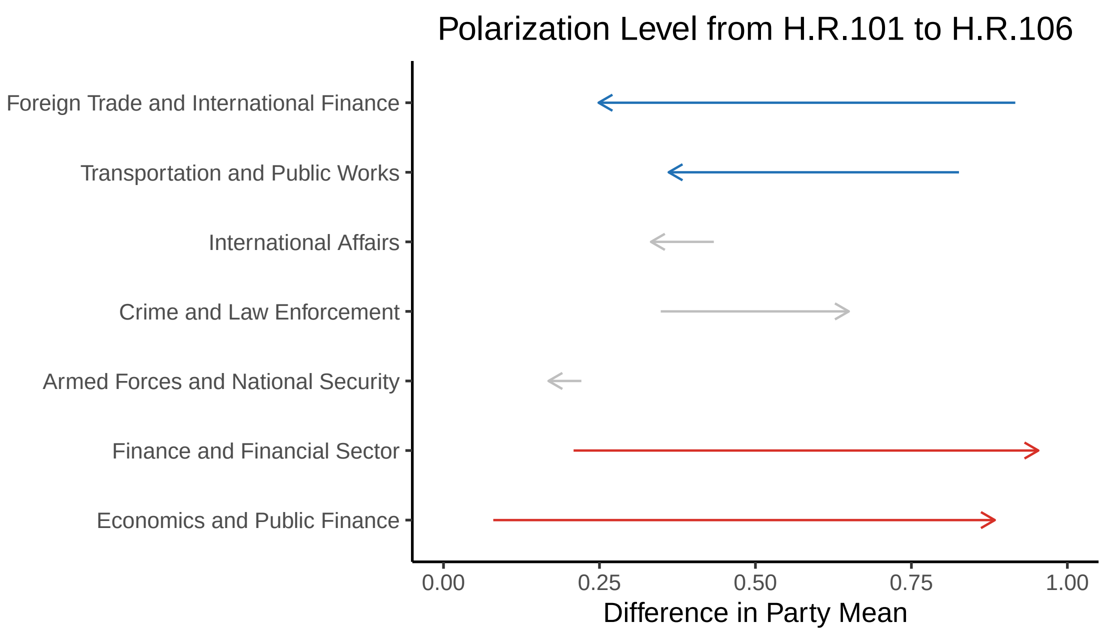

Figure 9: Change in polarization levels for selected issues during the 1990s. Each arrow connects the polarization level, measured as the difference in party means of dynamic issue-specific ideal point estimates, from 101st H.R. (1989–1990) to 106th H.R. (1999–2000) for each issue area. The top two arrows (blue) represent issue areas with decreased polarization, while the bottom two arrows (red) represent those with increased polarization. The three arrows (grey) represent issue areas with relatively modest changes.

Figures 10 and 11 trace the trajectory of polarization during the 1990s in greater detail, highlighting issue areas with marked change in polarization levels. First, we observe that polarization for private and public finance increased drastically during the first two years of the Gingrich Speakership. The imprint of the 1995-1996 federal government shutdowns is indicated in the sharp jump of the green line in Figure 10. Second, we observe that polarization for international trade and finance decreased drastically during the years surrounding the 1992 elections. The most likely explanation here is the change of policy substance ushered in by the end of the Cold War. As trade became less of an issue of ideology, intraparty differences based on economic interests substituted partisan differences as the most salient cleavage, thereby lowering the partisan polarization level.

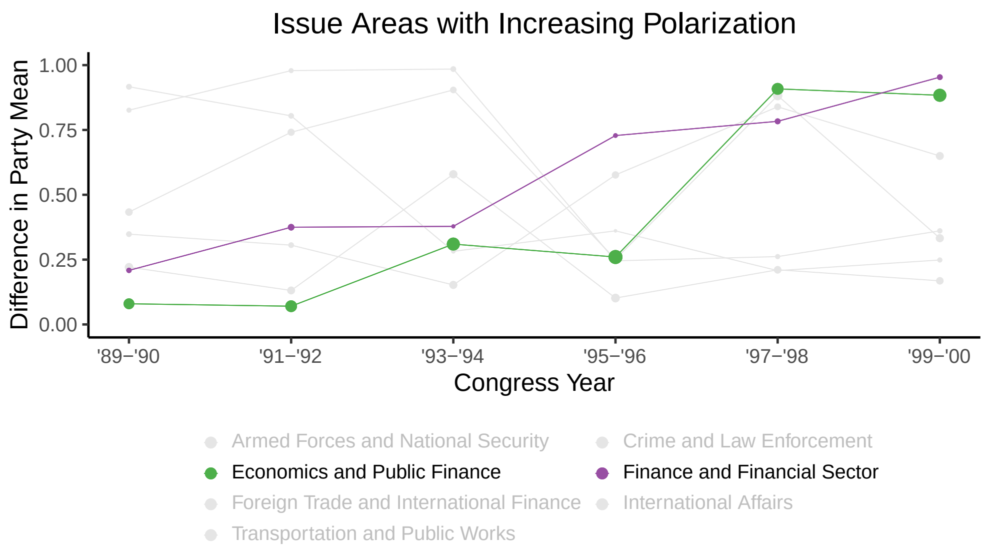

Figure 10: Trajectory of polarization levels for issues with increasing polarization during the 1990s. Each line represents the polarization level, measured as the difference in party means of dynamic issue-specific ideal point estimates, for each issue area over time. The size of the dots is proportional to the number of roll calls.

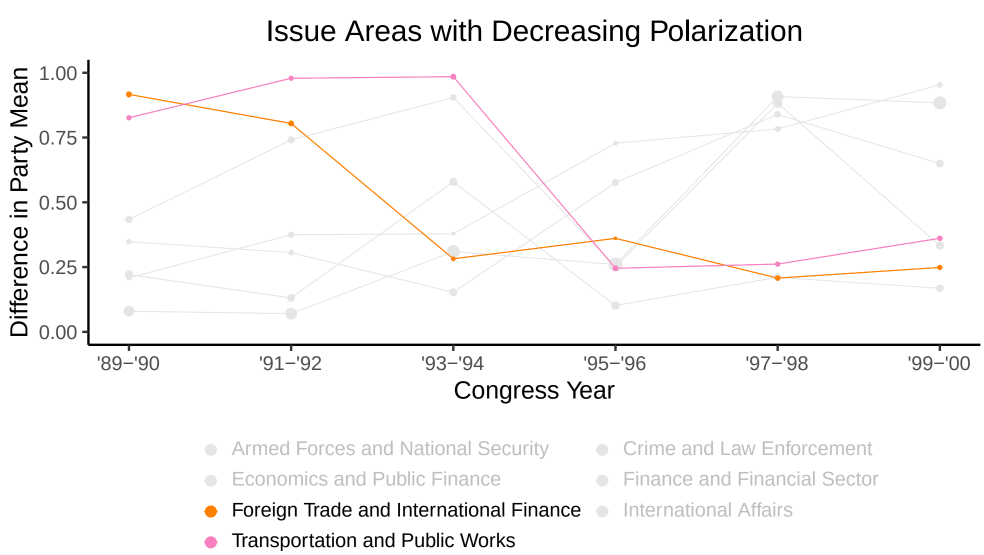

Figure 11: Trajectory of polarization levels for issues with decreasing polarization during the 1990s. Each line represents the polarization level, measured as the difference in party means of dynamic issue-specific ideal point estimates, for each issue area over time. The size of the dots is proportional to the number of roll calls.

To further confirm our observation, Figure 12 compares the issue-specific axes for public finance (green) and foreign trade (orange) for the 102nd and the 106th Congresses. It shows that during the 102nd Congress, the trade-specific axis was mostly aligned with partisan lines, whereas public finance was not. A reversed pattern is observed in the 106th Congress, demonstrating a different trajectory of polarization in these two issue areas. See Appendix E.2.3 for the trend in its entirety, from 1991 to 2000.

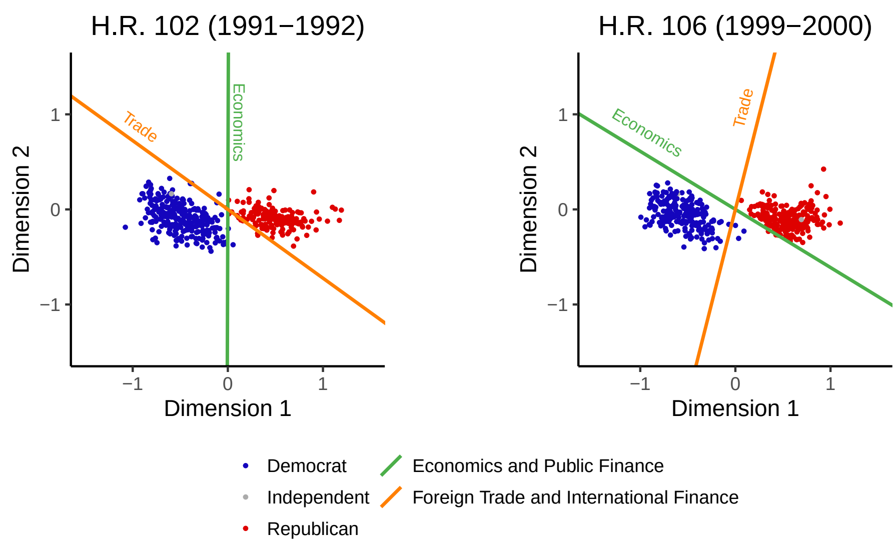

Figure 12: Comparison between public finance-specific (green) and foreign trade-specific axes (orange) for the 102nd and 106th H.R. Each dot represents the ideal points of representatives, with color indicating party affiliation (blue for Democrats; red for Republicans).

Together, the analysis using issue-specific ideal points shows that the polarization level has increased over time, with varying degrees depending on the issue areas. These results point toward opportunities for further analyses. We can, for instance, conduct a detailed study of a single legislator or a group of legislators, tracking the movement of their issue-specific ideal points. Another possible extension could test the "asymmetric polarization" thesis by policy issue, assessing each party's contribution to the widening difference in party means (Hacker and Pierson, 2015). A further extension might compare issue-specific polarization levels between the two chambers of Congress, interrogating how one influences the other (Theriault, 2013).

6 Concluding Remarks

Ideal points have been widely used for measuring ideology, yet their nature as a latent space makes it difficult to target specific issue areas of interest. In this paper, I proposed a hierarchical IRT model based on classic spatial voting theory that provides a measure of issue axes and issue-specific ideal points. Unlike the common practice of using only a subset of data, the proposed method leverages information from the entire set of voting data. More importantly, using this method, scholars can compare the similarity of different issue areas in terms of their left-to-right alignment.

I demonstrated that the proposed method effectively captures issue-specific voting behaviors through simulations and two application studies of the US House of Representatives. First, I revisited the Battle of the Standards during the 1890s and showed that the proposed method successfully captures the sectional alignment over monetary policy: Southern Democrats and the Populists from the West versus Northeastern representatives (Bensel, 2000; Frieden, 2016). Second, I found that polarization levels have increased over time across issue areas, with varying degrees. These findings suggest that the proposed method is a powerful tool for analyzing legislative behavior, offering an in-depth understanding of issue-specific ideologies and their dynamics over time.

Future extensions of the model include generalizing issue-label parameters to incorporate more roll-call level covariates. This would allow us to model the roll-call specific mean direction vector as $\boldsymbol{u}_j \sim \text{vMF}_d(f(\boldsymbol{X}_j), \rho)$, leveraging a wide range of data, including the text of bills, and enabling the use of multiple issue labels for a single roll-call (e.g., political economy and election-related roll-call). Additionally, we can model issue-specific dispersion of directions by using ρ_z instead of ρ in $\boldsymbol{u}_j \sim \text{vMF}_d(\boldsymbol{\theta}_{z_j}, \rho_{z_j})$, allowing different levels of deviation of roll-calls from their issue-specific axis depending on the policy area. For example, roll-calls concerning political economy issues could vary more compared to those of election issues. Finally, the model can be extended to other types of data, including survey responses, as a measurement tool for capturing latent concepts with user-specified factors.

References

Bafumi, Joseph and Michael C Herron. 2010. "Leapfrog representation and extremism: A study of American voters and their members in Congress." *American Political Science Review* 104(3):519–542.

Bailey, Michael A, Anton Strezhnev and Erik Voeten. 2017. "Estimating dynamic state preferences from United Nations voting data." *Journal of Conflict Resolution* 61(2):430–456.

Bailey, Michael and Kelly H Chang. 2001. "Comparing presidents, senators, and justices: interinstitutional preference estimation." *Journal of Law, Economics, and Organization* 17(2):477–506.

Barberá, Pablo. 2015. "Birds of the same feather tweet together: Bayesian ideal point estimation using Twitter data." *Political Analysis* 23(1):76–91.

Bateman, David A, Ira Katznelson and John S Lapinski. 2022. Issue codings for roll call in the U.S. House of Representatives and Senate between 1877 and 2011. Technical report American Institutions Project. http://www.davidalexbateman.net/congressional-data.html.

Bateman, David A, Joshua D Clinton and John S Lapinski. 2017. "A house divided? roll calls, polarization, and policy differences in the us house, 1877–2011." *American Journal of Political Science* 61(3):698–714.

Bensel, Richard Franklin. 2000. *The political economy of American industrialization, 1877–1900.* Cambridge University Press.

Binding, Garret and Lukas F Stoetzer. 2022. "Non-Separable Preferences in the Statistical Analysis of Roll Call Votes." *Political Analysis* pp. 1–14.

Bond, Robert and Solomon Messing. 2015. "Quantifying social media's political space: Estimating ideology from publicly revealed preferences on Facebook." *American Political Science Review* 109(1):62–78.

Bonica, Adam. 2014. "Mapping the ideological marketplace." *American Journal of Political Science* 58(2):367–386.

Carroll, Royce, Jeffrey B Lewis, James Lo, Keith T Poole and Howard Rosenthal. 2013. "The Structure of Utility in Spatial Models of Voting." *American Journal of Political Science* 57(4):1008–1028.

Clinton, Joshua, Simon Jackman and Douglas Rivers. 2004. "The Statistical Analysis of Roll Call Data." *American Political Science Review* 98(2):355–370.

CRS, (Congressional Research Service). 2022. 32 policy area terms. Technical report Congress.gov. https://www.congress.gov/help/field-values/policy-area.

Frieden, Jeffry A. 2016. *Currency politics: The political economy of exchange rate policy*. Princeton University Press.

Gerrish, Sean and David Blei. 2012. "How they vote: Issue-adjusted models of legislative behavior." *Advances in neural information processing systems* 25.

Gerrish, Sean M and David M Blei. 2011. Predicting legislative roll calls from text. In *Proceedings of the 28th International Conference on Machine Learning, ICML 2011*.

Goplerud, Max. 2019. "A Multinomial Framework for Ideal Point Estimation." *Political Analysis* 27(1):69–89.

Hacker, Jacob S and Paul Pierson. 2015. "Confronting asymmetric polarization." *Solutions to political polarization in America* 59:66.

Hill, Seth J and Chris Tausanovitch. 2015. "A disconnect in representation? Comparison of trends in congressional and public polarization." *The Journal of Politics* 77(4):1058–1075.

Hix, Simon, Abdul Noury and Gerard Roland. 2006. "Dimensions of politics in the European Parliament." *American Journal of Political Science* 50(2):494–520.

Hoff, Peter D. 2007. "Model Averaging and Dimension Selection for the Singular Value Decomposition." *Journal of the American Statistical Association* 102(478):674–685.
URL: *https://doi.org/10.1198/016214506000001310*

Hoff, Peter D. 2009. "Simulation of the Matrix Bingham–von Mises–Fisher Distribution, With Applications to Multivariate and Relational Data." *Journal of Computational and Graphical Statistics* 18(2):438–456.
URL: *https://doi.org/10.1198/jcgs.2009.07177*

Imai, Kosuke, James Lo and Jonathan Olmsted. 2016. "Fast estimation of ideal points with massive data." *American Political Science Review* 110(4):631–656.

Iyengar, Shanto, Yphtach Lelkes, Matthew Levendusky, Neil Malhotra and Sean J Westwood. 2019. "The origins and consequences of affective polarization in the United States." *Annual Review of Political Science* 22(1):129–146.

Jackman, Simon. 2001. "Multidimensional analysis of roll call data via Bayesian simulation: Identification, estimation, inference, and model checking." *Political Analysis* 9(3):227–241.

Jackman, Simon. 2020. *pscl: Classes and Methods for R Developed in the Political Science Computational Laboratory*. Sydney, New South Wales, Australia: United States Studies Centre, University of Sydney. R package version 1.5.5.
URL: *https://github.com/atahk/pscl/*

Jeong, Gyung-Ho. 2018. "Measuring foreign policy positions of members of the US congress." *Political Science Research and Methods* 6(1):181–196.

Jones, Bryan D., Frank R. Baumgartner, Sean M. Theriault, Derek A. Epp, Cheyenne Lee, Miranda E. Sullivan and Chris Cassella. 2023. "Policy Agendas Project: Codebook.".
URL: *https://www.comparativeagendas.net*

Katznelson, Ira and John S Lapinski. 2006. The substance of representation: studying policy content and legislative behavior. In *The Macropolitics of Congress*. Princeton University Press Princeton, NJ pp. 96–126.

Lauderdale, Benjamin E and Tom S Clark. 2014. "Scaling politically meaningful dimensions using texts and votes." *American Journal of Political Science* 58(3):754–771.

Layman, Geoffrey C, Thomas M Carsey and Juliana Menasce Horowitz. 2006. "Party polarization in American politics." *Annual Review of Political Science* 9:83–110.

Lee, Frances E. 2015. "How party polarization affects governance." *Annual review of political science* 18(1):261–282.

Lewis, Jeffrey B., Keith Poole, Howard Rosenthal, Adam Boche, Aaron Rudkin and Luke Sonnet. 2022. Voteview: Congressional Roll-Call Votes Database. Technical report.
URL: *https://voteview.com/*

Marble, William and Matthew Tyler. 2021. "The Structure of Political Choices: Distinguishing Between Constraint and Multidimensionality." *Political Analysis* pp. 1–18.

Martin, Andrew D and Kevin M Quinn. 2002. "Dynamic ideal point estimation via Markov chain Monte Carlo for the US Supreme Court, 1953–1999." *Political Analysis* 10(2):134–153.

McAlister, Kevin. 2021. "Disagreement and Dimensionality: A Varying Dimensions Approach to Roll Call Scaling in the US Congress." Unpublished manuscript.

McCarty, Nolan, Keith T Poole and Howard Rosenthal. 2006. *Polarized America: The dance of ideology and unequal riches*. MIT Press.

Morucci, Marco, Margaret Foster, Kaitlyn Webster, So Jin Lee and David Siegel. 2024. "Measurement That Matches Theory: Theory-Driven Identification in Item Response Theory Models." *American Political Science Review* p. 1–19.

Moser, Scott, Abel Rodríguez and Chelsea L Lofland. 2021. "Multiple ideal points: Revealed preferences in different domains." *Political Analysis* 29(2):139–166.

Peress, Michael. 2013. "Estimating Proposal and Status Quo Locations Using Voting and Cosponsorship Data." *The Journal of Politics* 75(3):613–631.
URL: *https://doi.org/10.1017/S0022381613000571*

Peress, Michael. 2020. "Large-Scale Ideal Point Estimation." *Political Analysis* pp. 1–18.

Poole, Keith, Jeffrey Lewis, James Lo and Royce Carroll. 2011. "Scaling Roll Call Votes with wnominate in R." *Journal of Statistical Software* 42(14):1–21.
URL: *https://www.jstatsoft.org/v42/i14/*

Poole, Keith T. and Howard Rosenthal. 1997. *Congress: A Political-Economic History of Roll-Call Voting*. Oxford: Oxford University Press.

Pourzanjani, Arya A, Richard M Jiang, Brian Mitchell, Paul J Atzberger and Linda R Petzold. 2021. "Bayesian inference over the Stiefel manifold via the Givens representation." *Bayesian Analysis* 16(2):639–666.

Rivers, Douglas. 2003. "Identification of multidimensional item-response models." *Typescript. Department of Political Science, Stanford University* .

Shor, Boris and Nolan McCarty. 2011. "The ideological mapping of American legislatures." *American Political Science Review* 105(3):530–551.

Slapin, Jonathan B and Sven-Oliver Proksch. 2008. "A scaling model for estimating time-series party positions from texts." *American Journal of Political Science* 52(3):705–722.

Sohn, Yunkyu. 2017. *Measuring Ideology, Dimensionality and Polarization in Politics.* University of California, San Diego.

Stan Development Team. 2024. "RStan: the R interface to Stan.". R package version 2.32.5.
URL: *https://mc-stan.org/*

Straub, Julian. 2017. Bayesian inference with the von-Mises-Fisher distribution in 3d. Technical report. https://people.csail.mit.edu/jstraub/download/straub2017vonMisesFisherInference.pdf.

Tausanovitch, Chris and Christopher Warshaw. 2013. "Measuring constituent policy preferences in congress, state legislatures, and cities." *The Journal of Politics* 75(2):330–342.

Theriault, Sean M. 2013. *The Gingrich senators: The roots of partisan warfare in Congress.* Oxford University Press.

Vafa, Keyon, Suresh Naidu and David M Blei. 2020. "Text-based ideal points." *Proceedings of the 2020 Conference of the Association for Computational Linguistics, ACL 2020* .

Voeten, Erik. 2000. "Clashes in the Assembly." *International Organization* 54(2):185–215.

Voeten, Erik, Anton Strezhnev and Michael Bailey. 2009. "United Nations General Assembly Voting Data.".
URL: *https://doi.org/10.7910/DVN/LEJUQZ*

White, Richard. 2017. *The republic for which it stands: The United States during reconstruction and the gilded age, 1865-1896.* Oxford University Press.

You, Hye Young. 2022. "Dynamic lobbying: Evidence from foreign lobbying in the US Congress." *Economics & Politics* .

A Proofs

A.1 Proof of Proposition 1

Proof. Applying the Pythagorean theorem, we have

$$\|\boldsymbol{x}_i - \boldsymbol{o}_j^{\mathrm{n}}\|^2 = \|\mathrm{proj}_{\boldsymbol{o}_j^{\mathrm{y}} - \boldsymbol{o}_j^{\mathrm{n}}}(\boldsymbol{x}_i - \boldsymbol{o}_j^{\mathrm{n}})\|^2 + \|\mathrm{oproj}_{\boldsymbol{o}_j^{\mathrm{y}} - \boldsymbol{o}_j^{\mathrm{n}}}(\boldsymbol{x}_i - \boldsymbol{o}_j^{\mathrm{n}})\|^2$$
$$\|\boldsymbol{x}_i - \boldsymbol{o}_j^{\mathrm{y}}\|^2 = \|\mathrm{proj}_{\boldsymbol{o}_j^{\mathrm{n}} - \boldsymbol{o}_j^{\mathrm{y}}}(\boldsymbol{x}_i - \boldsymbol{o}_j^{\mathrm{y}})\|^2 + \|\mathrm{oproj}_{\boldsymbol{o}_j^{\mathrm{n}} - \boldsymbol{o}_j^{\mathrm{y}}}(\boldsymbol{x}_i - \boldsymbol{o}_j^{\mathrm{y}})\|^2$$

where $\mathrm{oproj}_{\boldsymbol{a}}\boldsymbol{b}$ denotes the projection of $\boldsymbol{b}$ onto the orthogonal complement of $\boldsymbol{a}$. First we show that $\|\mathrm{proj}_{\boldsymbol{o}_j^{\mathrm{y}} - \boldsymbol{o}_j^{\mathrm{n}}}(\boldsymbol{x}_i - \boldsymbol{o}_j^{\mathrm{n}})\|^2$ can be simplified as follows:

$$\begin{aligned}
\|\mathrm{proj}_{\boldsymbol{o}_j^{\mathrm{y}} - \boldsymbol{o}_j^{\mathrm{n}}}(\boldsymbol{x}_i - \boldsymbol{o}_j^{\mathrm{n}})\|^2 &= \left\| \frac{(\boldsymbol{x}_i - \boldsymbol{o}_j^{\mathrm{n}})^\top (\boldsymbol{o}_j^{\mathrm{y}} - \boldsymbol{o}_j^{\mathrm{n}})}{\|\boldsymbol{o}_j^{\mathrm{y}} - \boldsymbol{o}_j^{\mathrm{n}}\|} (\boldsymbol{o}_j^{\mathrm{y}} - \boldsymbol{o}_j^{\mathrm{n}}) \right\|^2 \\
&= (\boldsymbol{x}_i - \boldsymbol{o}_j^{\mathrm{n}})^\top (\boldsymbol{o}_j^{\mathrm{y}} - \boldsymbol{o}_j^{\mathrm{n}}) \left\| \frac{\boldsymbol{o}_j^{\mathrm{y}} - \boldsymbol{o}_j^{\mathrm{n}}}{\|\boldsymbol{o}_j^{\mathrm{y}} - \boldsymbol{o}_j^{\mathrm{n}}\|} \right\|^2 \\
&= (\boldsymbol{x}_i - \boldsymbol{o}_j^{\mathrm{n}})^\top (\boldsymbol{o}_j^{\mathrm{y}} - \boldsymbol{o}_j^{\mathrm{n}})
\end{aligned}$$

Similarly,

$$\|\mathrm{proj}_{\boldsymbol{o}_j^{\mathrm{n}} - \boldsymbol{o}_j^{\mathrm{y}}}(\boldsymbol{x}_i - \boldsymbol{o}_j^{\mathrm{y}})\|^2 = (\boldsymbol{x}_i - \boldsymbol{o}_j^{\mathrm{y}})^\top (\boldsymbol{o}_j^{\mathrm{n}} - \boldsymbol{o}_j^{\mathrm{y}})$$

Now, we show that $\|\mathrm{oproj}_{\boldsymbol{o}_j^{\mathrm{y}} - \boldsymbol{o}_j^{\mathrm{n}}}(\boldsymbol{x}_i - \boldsymbol{o}_j^{\mathrm{n}})\|^2 = \|\mathrm{oproj}_{\boldsymbol{o}_j^{\mathrm{n}} - \boldsymbol{o}_j^{\mathrm{y}}}(\boldsymbol{x}_i - \boldsymbol{o}_j^{\mathrm{y}})\|^2$.

$$\begin{aligned}
\|\mathrm{oproj}_{\boldsymbol{o}_j^{\mathrm{y}} - \boldsymbol{o}_j^{\mathrm{n}}}(\boldsymbol{x}_i - \boldsymbol{o}_j^{\mathrm{n}})\|^2 &= \|\boldsymbol{x}_i - \boldsymbol{o}_j^{\mathrm{n}}\|^2 - \|\mathrm{proj}_{\boldsymbol{o}_j^{\mathrm{y}} - \boldsymbol{o}_j^{\mathrm{n}}}(\boldsymbol{x}_i - \boldsymbol{o}_j^{\mathrm{n}})\|^2 \\
&= \|\boldsymbol{x}_i - \boldsymbol{o}_j^{\mathrm{n}}\|^2 - (\boldsymbol{x}_i - \boldsymbol{o}_j^{\mathrm{n}})^\top (\boldsymbol{o}_j^{\mathrm{y}} - \boldsymbol{o}_j^{\mathrm{n}}) \\
&= (\boldsymbol{x}_i - \boldsymbol{o}_j^{\mathrm{n}})^\top (\boldsymbol{x}_i - \boldsymbol{o}_j^{\mathrm{n}}) - (\boldsymbol{x}_i - \boldsymbol{o}_j^{\mathrm{n}})^\top (\boldsymbol{o}_j^{\mathrm{y}} - \boldsymbol{o}_j^{\mathrm{n}}) \\
&= (\boldsymbol{x}_i - \boldsymbol{o}_j^{\mathrm{n}})^\top (\boldsymbol{x}_i - \boldsymbol{o}_j^{\mathrm{y}})
\end{aligned}$$

Similarly,

$$\begin{aligned}\|\mathrm{oproj}_{\boldsymbol{o}_j^{\mathrm{n}}-\boldsymbol{o}_j^{\mathrm{y}}}(\boldsymbol{x}_i-\boldsymbol{o}_j^{\mathrm{y}})\|^2 &= \|\boldsymbol{x}_i-\boldsymbol{o}_j^{\mathrm{y}}\|^2 - \|\mathrm{proj}_{\boldsymbol{o}_j^{\mathrm{n}}-\boldsymbol{o}_j^{\mathrm{y}}}(\boldsymbol{x}_i-\boldsymbol{o}_j^{\mathrm{y}})\|^2 \\ &= \|\boldsymbol{x}_i-\boldsymbol{o}_j^{\mathrm{y}}\|^2 - (\boldsymbol{x}_i-\boldsymbol{o}_j^{\mathrm{y}})^\top(\boldsymbol{o}_j^{\mathrm{n}}-\boldsymbol{o}_j^{\mathrm{y}}) \\ &= (\boldsymbol{x}_i-\boldsymbol{o}_j^{\mathrm{y}})^\top(\boldsymbol{x}_i-\boldsymbol{o}_j^{\mathrm{y}}) - (\boldsymbol{x}_i-\boldsymbol{o}_j^{\mathrm{y}})^\top(\boldsymbol{o}_j^{\mathrm{n}}-\boldsymbol{o}_j^{\mathrm{y}}) \\ &= (\boldsymbol{x}_i-\boldsymbol{o}_j^{\mathrm{y}})^\top(\boldsymbol{x}_i-\boldsymbol{o}_j^{\mathrm{n}})\end{aligned}$$

Therefore, we have $\|\mathrm{oproj}_{\boldsymbol{o}_j^{\mathrm{y}}-\boldsymbol{o}_j^{\mathrm{n}}}(\boldsymbol{x}_i-\boldsymbol{o}_j^{\mathrm{n}})\|^2 = \|\mathrm{oproj}_{\boldsymbol{o}_j^{\mathrm{n}}-\boldsymbol{o}_j^{\mathrm{y}}}(\boldsymbol{x}_i-\boldsymbol{o}_j^{\mathrm{y}})\|^2$. Using the Pythagorean theorem, this implies that

$$\begin{aligned}\|\boldsymbol{x}_i-\boldsymbol{o}_j^{\mathrm{n}}\|^2 - \|\boldsymbol{x}_i-\boldsymbol{o}_j^{\mathrm{y}}\|^2 &= \|\mathrm{proj}_{\boldsymbol{o}_j^{\mathrm{y}}-\boldsymbol{o}_j^{\mathrm{n}}}(\boldsymbol{x}_i-\boldsymbol{o}_j^{\mathrm{n}})\|^2 + \|\mathrm{oproj}_{\boldsymbol{o}_j^{\mathrm{y}}-\boldsymbol{o}_j^{\mathrm{n}}}(\boldsymbol{x}_i-\boldsymbol{o}_j^{\mathrm{n}})\|^2 \\ &\quad - \|\mathrm{proj}_{\boldsymbol{o}_j^{\mathrm{n}}-\boldsymbol{o}_j^{\mathrm{y}}}(\boldsymbol{x}_i-\boldsymbol{o}_j^{\mathrm{y}})\|^2 - \|\mathrm{oproj}_{\boldsymbol{o}_j^{\mathrm{n}}-\boldsymbol{o}_j^{\mathrm{y}}}(\boldsymbol{x}_i-\boldsymbol{o}_j^{\mathrm{y}})\|^2 \\ &= \|\mathrm{proj}_{\boldsymbol{o}_j^{\mathrm{y}}-\boldsymbol{o}_j^{\mathrm{n}}}(\boldsymbol{x}_i-\boldsymbol{o}_j^{\mathrm{n}})\|^2 - \|\mathrm{proj}_{\boldsymbol{o}_j^{\mathrm{n}}-\boldsymbol{o}_j^{\mathrm{y}}}(\boldsymbol{x}_i-\boldsymbol{o}_j^{\mathrm{y}})\|^2\end{aligned}$$

Plugging this result to the Equation (1), we have

$$\begin{aligned}\Pr(y_{ij}=1) &= \Phi\left(\|\boldsymbol{x}_i-\boldsymbol{o}_j^{\mathrm{n}}\|^2 - \|\boldsymbol{x}_i-\boldsymbol{o}_j^{\mathrm{y}}\|^2\right) \\ &= \Phi\left(\|\mathrm{proj}_{\boldsymbol{o}_j^{\mathrm{y}}-\boldsymbol{o}_j^{\mathrm{n}}}(\boldsymbol{x}_i-\boldsymbol{o}_j^{\mathrm{n}})\|^2 - \|\mathrm{proj}_{\boldsymbol{o}_j^{\mathrm{n}}-\boldsymbol{o}_j^{\mathrm{y}}}(\boldsymbol{x}_i-\boldsymbol{o}_j^{\mathrm{y}})\|^2\right)\end{aligned}$$

□

A.2 Remark of Proposition 1

Remark 1 (Factorization of the discrimination parameter)**.** Observe that

$$\begin{aligned}\Pr(y_{ij}=1) &= \Phi\left(\|\mathrm{proj}_{\boldsymbol{o}_j^{\mathrm{y}}-\boldsymbol{o}_j^{\mathrm{n}}}(\boldsymbol{x}_i-\boldsymbol{o}_j^{\mathrm{n}})\|^2 - \|\mathrm{proj}_{\boldsymbol{o}_j^{\mathrm{n}}-\boldsymbol{o}_j^{\mathrm{y}}}(\boldsymbol{x}_i-\boldsymbol{o}_j^{\mathrm{y}})\|^2\right) \\ &= \Phi\left((\boldsymbol{x}_i-\boldsymbol{o}_j^{\mathrm{n}})^\top(\boldsymbol{o}_j^{\mathrm{y}}-\boldsymbol{o}_j^{\mathrm{n}}) - (\boldsymbol{x}_i-\boldsymbol{o}_j^{\mathrm{y}})^\top(\boldsymbol{o}_j^{\mathrm{n}}-\boldsymbol{o}_j^{\mathrm{y}})\right) \\ &= \Phi\left(2(\boldsymbol{o}_j^{\mathrm{y}}-\boldsymbol{o}_j^{\mathrm{n}})^\top\boldsymbol{x}_i - (\boldsymbol{o}_j^{\mathrm{y}\top}\boldsymbol{o}_j^{\mathrm{y}} - \boldsymbol{o}_j^{\mathrm{n}\top}\boldsymbol{o}_j^{\mathrm{n}})\right) \\ &= \Phi\left(\|2(\boldsymbol{o}_j^{\mathrm{y}}-\boldsymbol{o}_j^{\mathrm{n}})\|\underbrace{\frac{(\boldsymbol{o}_j^{\mathrm{y}}-\boldsymbol{o}_j^{\mathrm{n}})}{\|(\boldsymbol{o}_j^{\mathrm{y}}-\boldsymbol{o}_j^{\mathrm{n}})\|}^\top}_{\substack{\text{Nay-to-Yea} \\ \text{direction}}}\boldsymbol{x}_i - (\boldsymbol{o}_j^{\mathrm{y}\top}\boldsymbol{o}_j^{\mathrm{y}} - \boldsymbol{o}_j^{\mathrm{n}\top}\boldsymbol{o}_j^{\mathrm{n}})\right)\end{aligned}$$

The last line implies that the discrimination parameter $2(\boldsymbol{o}_j^{\mathrm{y}} - \boldsymbol{o}_j^{\mathrm{n}})$ can be factored into two terms, where the second term corresponds to the Nay-to-Yea direction of the roll-call specific axis. Based on this factorization, I build a hierarchical model on the second term, enabling us to estimate the direction of the issue-specific axis.

A.3 Proof of Property 1

Proof.

$$\begin{aligned}
y_{ij}^* &\equiv w_j \boldsymbol{\theta}_{z_j}^\top (x_i^*(z_j) \boldsymbol{\theta}_{z_j}) - \alpha_j \\
&= w_j \boldsymbol{\theta}_{z_j}^\top \boldsymbol{\theta}_{z_j} \boldsymbol{\theta}_{z_j}^\top \boldsymbol{x}_i - \alpha_j \\
&= w_j \boldsymbol{\theta}_{z_j}^\top \boldsymbol{x}_i - \alpha_j \\
&= \mathbb{E}_{\boldsymbol{u}_j}[\mathbf{1}\{y_{ij} = 1\} \mid \boldsymbol{\theta}_{z_j}, w_j, \boldsymbol{x}_i, \alpha_j].
\end{aligned}$$

□

B Illustration of the Advantage of Using the Entire Dataset with a Simple Example

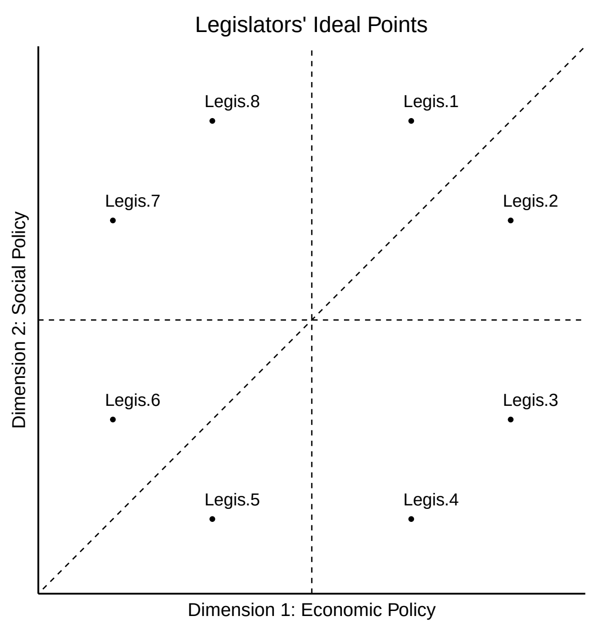

Figure 13: A toy example of two-dimensional ideal points.

Legislator	1	2	3	4	5	6	7	8
Economic Issue	0	0	0	0	1	1	1	1
Social Issue	0	0	1	1	1	1	0	0
Socio-Economic Issue	0	0	0	1	1	1	1	0

Table 2: A toy example of roll-call votes with three legislators and three issue areas. Here, 1 denotes liberal vote and 0 denotes conservative vote. Legislators 1 to 4, who are located right side of the Dimension 1 voted conservative on Economic issue, while the other legislators voted liberal. Similarly, Legislators 1,2,7, and 8 who are located at the top of the Dimension 2 voted conservative, while others voted liberal. On the Socio-Economic issue, legislators 1,2,3, and 8 voted conservative.

Here, I elaborate further on what it means to "borrow the information" from the roll-call votes of correlated issues. Suppose there are three legislators and three issue areas. Since the 'Economic' issue is correlated with the 'Socio-Economic' issue in terms of voting behavior, knowing how one voted on such a roll call gives us information about their preference, thus affecting how we should posit their ideal points. However, observe that voting behavior on the 'Social' issue is perfectly uncorrelated with that on the 'Economic' issue (the correlation of the second and third rows of Table 2 is zero). Therefore, we can posit the ideal points of legislators on the 'Social' issue without considering their voting behavior on the 'Economic' issue. In other words, in Figure 13, changing the second coordinate of the ideal points does not affect how one votes on the 'Economic' issue, since those two axes are orthogonal. This suggests the idea of borrowing information from correlated issues, while no information is shared between issues that are completely uncorrelated.

C Stan Code

```
data {
 int<lower=1> J; // Legislators
 int<lower=1> M; // Roll calls
 int<lower=1> N; // Num of observations (< M*J)
 int<lower=1> N_obs; // Num of observed
 int<lower=1> N_mis; // Num of missing
 int<lower=1> K; // Number of unique issues codes
 int<lower=1, upper=J> j[N]; // Legislator for observation n
 int<lower=1, upper=M> m[N]; // Roll call for observation n
 int<lower=0, upper=1> y_obs[N_obs]; // Vote of observation n
```

```
 int<lower=1> idx_obs[N_obs]; // Index of observed
 int<lower=1> idx_mis[N_mis]; // Index of missing
 int<lower=1, upper=K> z[M]; // Issue codes for roll call m
 real<lower=0> a; // Hyperparameter for rho
 real<lower=0> b; // Hyperparameter for theta
 // real<lower=0> rho;
}
parameters {
  real alpha[M]; // Difficulty of roll call m i.e. alpha_j = (O_yj'O_yj - O_nj'
     ↪ O_nj)/sigma_j
  real<lower=0> w[M]; // Scale for discrimination parameter
  real x_coord_theta[K]; // Issue vector in x,y-coordinates
  real y_coord_theta[K];
  real x_coord_u[M]; // Roll call vector in x,y-coordinates
  real y_coord_u[M];
  row_vector[2] x[J]; // Ideal point of legislator j
  real<lower=0> rho; // Concentration parameter
}
transformed parameters {
  real<lower=0> r_theta[K]; // Auxiliary variable for theta
  real theta[K]; // Issue vector in angle
  real<lower=0> r_u[M]; // Auxiliary variable for u
  real u[M]; // Roll call vector in angle
  for (k in 1:K) { // change from x,y-coordinates to polar coordinates
    theta[k] = atan2(y_coord_theta[k], x_coord_theta[k]);
    r_theta[k] = hypot(x_coord_theta[k], y_coord_theta[k]);
  }
  for (i in 1:M) { // change from x,y-coordinates to polar coordinates
    u[i] = atan2(y_coord_u[i], x_coord_u[i]);
    r_u[i] = hypot(x_coord_u[i], y_coord_u[i]);
  }
}
```

```
model {
  for (k in 1:J) { // Ideal point
    x[k][1] ~ normal(0,1);
    x[k][2] ~ normal(0,1);
  }
  target += -a*log(modified_bessel_first_kind(0, rho)); // Prior for rho
  for (k in 1:K) {
    r_theta[k] ~ normal(1.0, 0.1); // Sample auxiliary variable
    target += -log(r_theta[k]); // Log of determinant of Jacobian of Cartesian (x
        ↪ ,y) -> Polar (theta, r)
    // (i.e. determinanot of matrix of dr/dx, dr/dy, dtheta/dx, dtheta/dy)
    theta[k] ~ von_mises(0, b*rho); // Sample issue vector
  }
  for (i in 1:M) {
    r_u[i] ~ normal(1.0, 0.1); // Sample auxiliary variable
    target += -log(r_u[i]);
    u[i] ~ von_mises(theta[z[i]], rho); // Sample roll call vector
    w[i] ~ normal(0,5)T[0,]; // Scale parameter
    alpha[i] ~ normal(0,5); // Difficulty parameter
  }
  for (n in 1:N_obs) { // Sample observed votes
    y_obs[n] ~ bernoulli(Phi(dot_product(x[j[idx_obs[n]]], [cos(u[m[idx_obs[n]]])
        ↪ , sin(u[m[idx_obs[n]]])]) * w[m[idx_obs[n]]] - alpha[m[idx_obs[n]]]));
  }
}
generated quantities { // (Optional) Impute missing data using fitted parameters
  int<lower=0, upper=1> y_mis[N_mis];
  for (n in 1:N_mis) { // Impute missing votes
    y_mis[n] = bernoulli_rng(Phi(dot_product(x[j[idx_mis[n]]], [cos(u[m[idx_mis[n
        ↪ ]]]), sin(u[m[idx_mis[n]]])]) * w[m[idx_mis[n]]] - alpha[m[idx_mis[n
        ↪ ]]]));
  }
```

```
}
```

D Additional Results in Simulation Studies

D.1 Scenario 1: Correctly Specified Issue Codes

We consider a scenario with twelve different issue areas, as visualized in Figure 14. The results in Figure 15 demonstrate that the issue-specific ideal points estimated with our proposed method (top) align well with the true parameters, compared to the subsetting approach (bottom). The computation time and convergence metrics are presented in Table 3 and Tables 4 and 5.

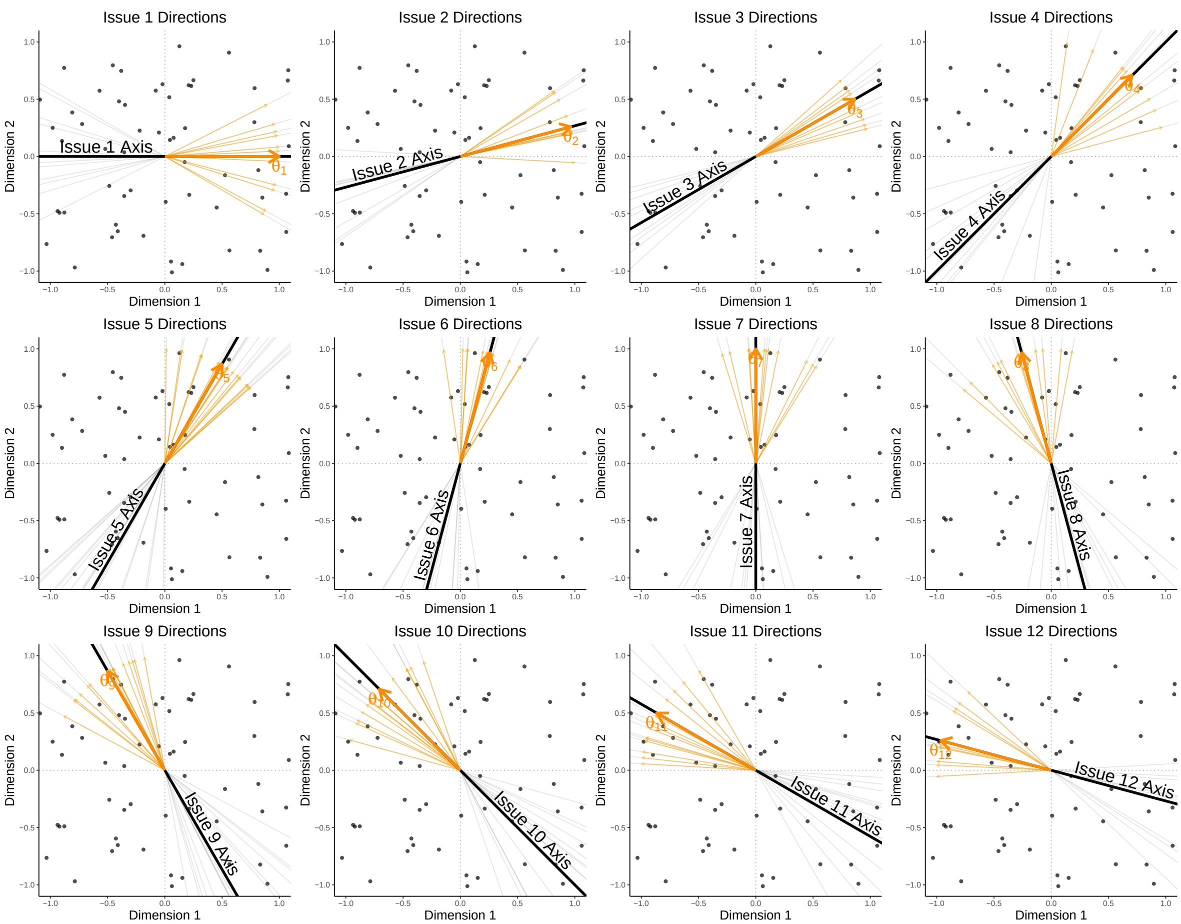

Figure 14: Issue-specific directions and ideal points used to generate synthetic data (Scenario 1).

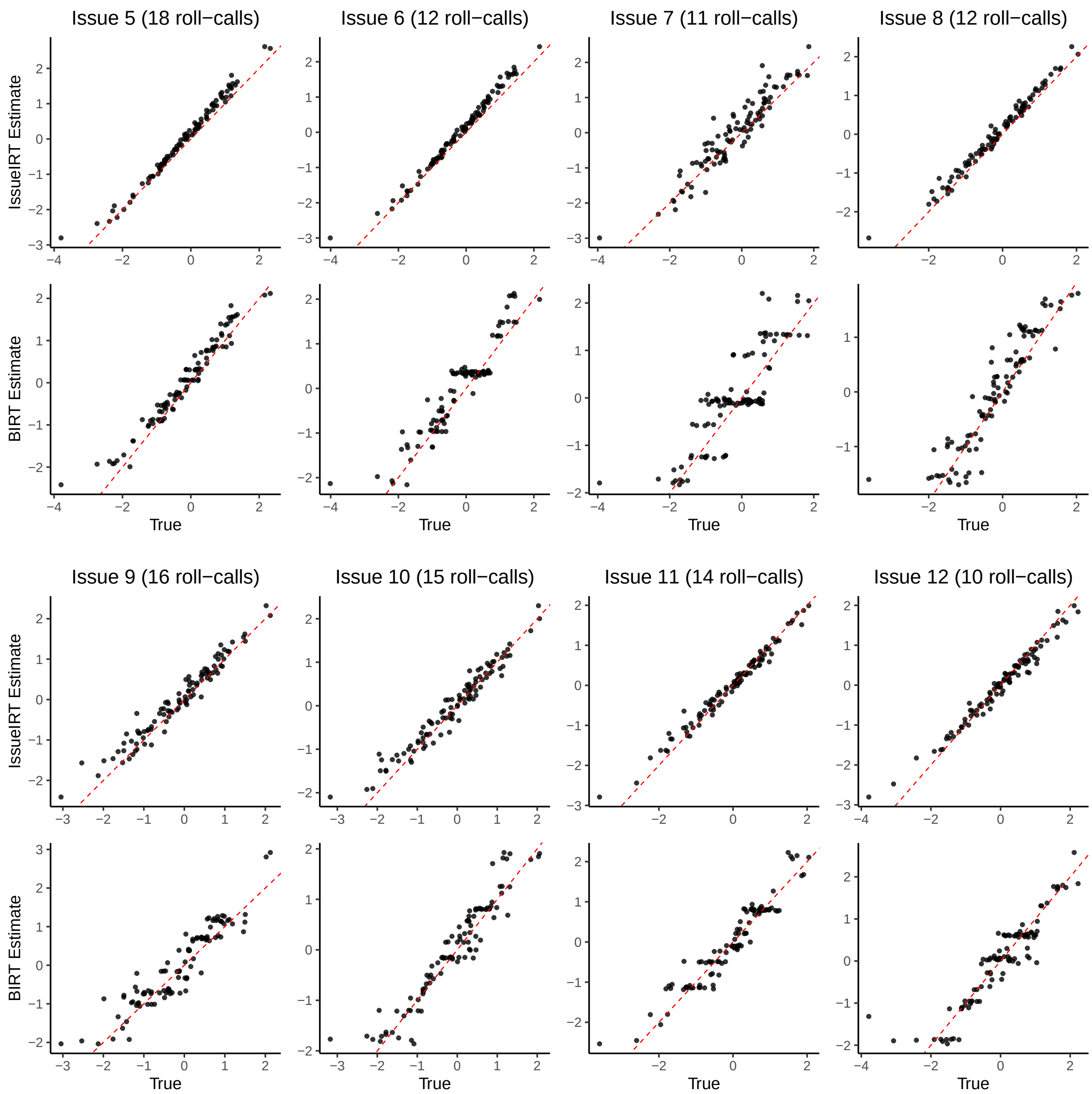

Figure 15: Estimation of issue-specific ideal points for the remaining eight issue areas (Scenario 1). Note that the signs of the `BIRT` estimates are adjusted for ease of comparison. In the original `BIRT` estimates, the ideal points for issues 1 to 9 have been flipped.

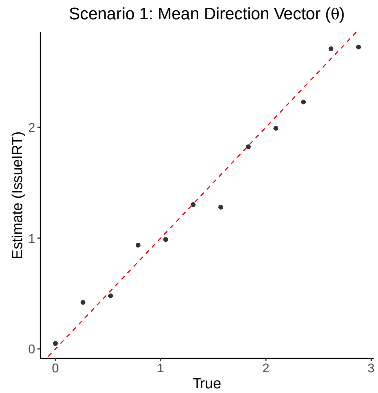

Figure 16: Estimation of issue specific mean direction vector (θ), transformed into angle (Scenario 1). Three legislators were anchored to address rotational invariance for ease of comparison.

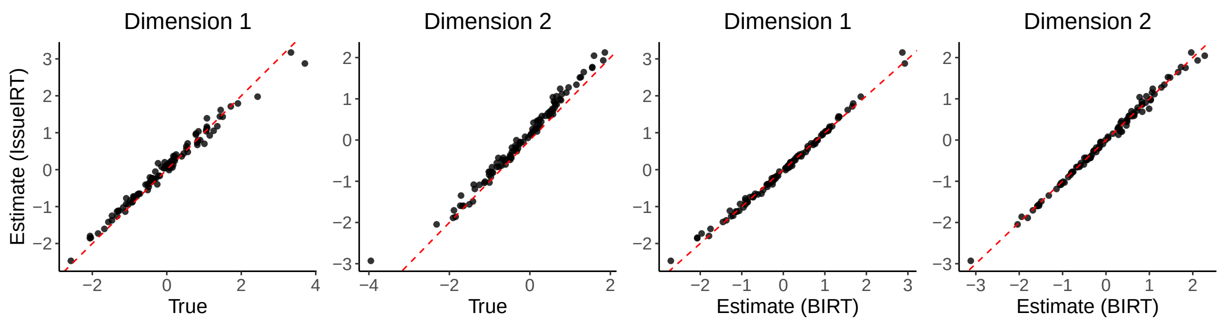

Figure 17: Estimation of multidimensional ideal points (Scenario 1). Three legislators were anchored to address rotational invariance for ease of comparison.

Chain	Warmup (mins)	Sampling (mins)
1	11.20	5.65
2	15.25	11.42

Table 3: Computation time with 2 chains, $1,000$ warmup, and $2,000$ samples (Scenario 1).

Parameter	Min of $\hat{R}$	25% of $\hat{R}$	Median of $\hat{R}$	75% of $\hat{R}$	Max of $\hat{R}$	Mean of $\hat{R}$
x_{i1}	1	1	1	1	1	1
x_{i2}	1	1	1	1	1	1
θ_z	1	1	1	1	1	1
u_j	1	1	1	1	1	1

Table 4: Summary of convergence diagnostics ($\hat{R}$) for the simulation study (Scenario 1).

Parameter	Min of ESS	25% of ESS	Median of ESS	75% of ESS	Max of ESS	Mean of ESS
x_{i1}	1483	1769	1880	1961	2130	1871
x_{i2}	1566	1729	1839	1910	2100	1823
θ_z	1697	1839	1921	2005	2133	1921
u_j	1597	1843	1924	1995	2182	1916

Table 5: Summary of effective sample size (ESS) for the simulation study (Scenario 1).

D.2 Scenario 2: Misspecified Issue Codes

We consider a hypothetical scenario in which the researcher mistakenly uses a more granular issue categorization. For example, as visualized in Figure 18, issues 1 to 4 (top), 5 to 8 (middle), and 9 to 12 (bottom) share the same issue axis, implying that these can be categorized into issues A, B, and C. That is, we assume the researcher considers a more granular categorization within each of issues A, B, and C. The results in Figure 19, 20, and 21 demonstrate that issue-specific ideal points estimated with our proposed method (top) align well with the true parameters, compared to the subsetting approach (bottom). The computation time and convergence metrics are presented in Table 6 and Tables 7 and 8.

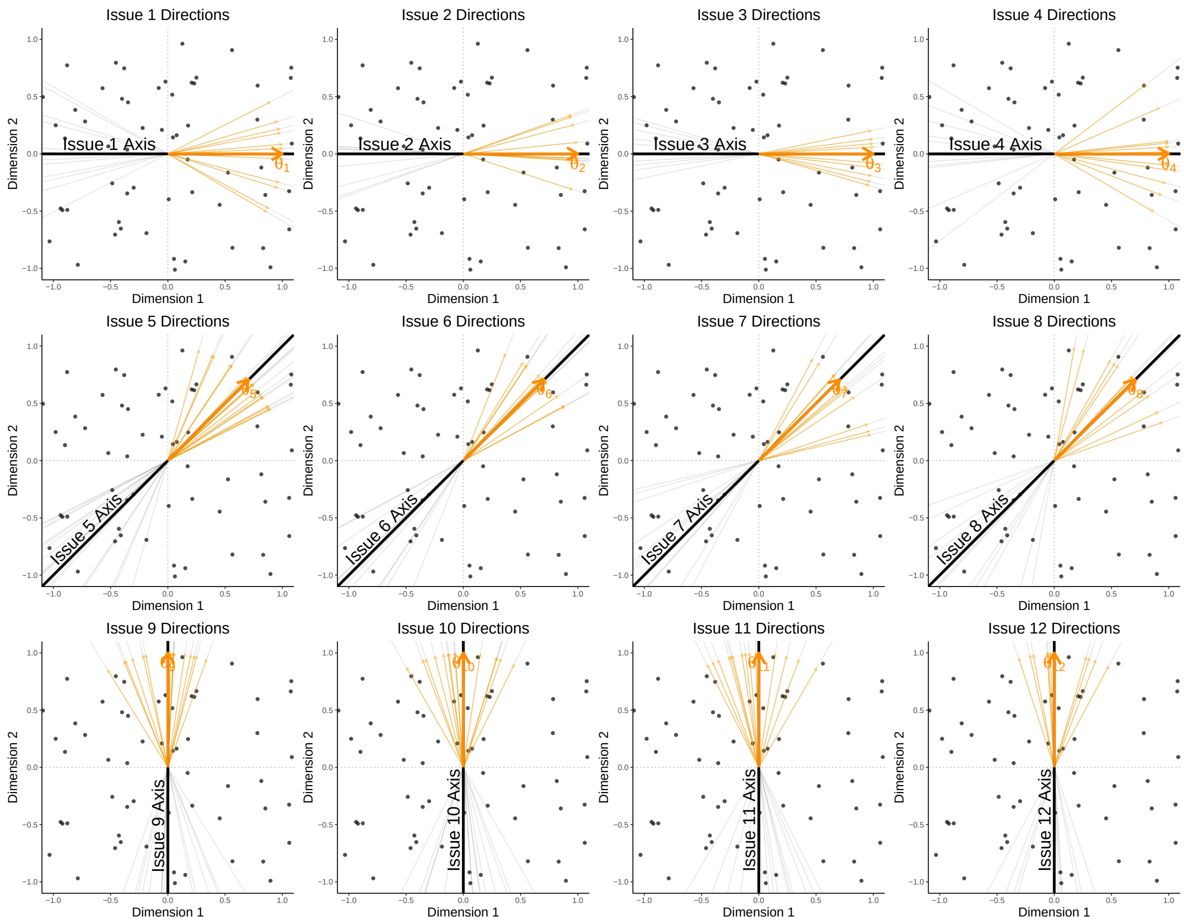

Figure 18: Issue-specific directions and ideal points used to generate synthetic data (Scenario 2).

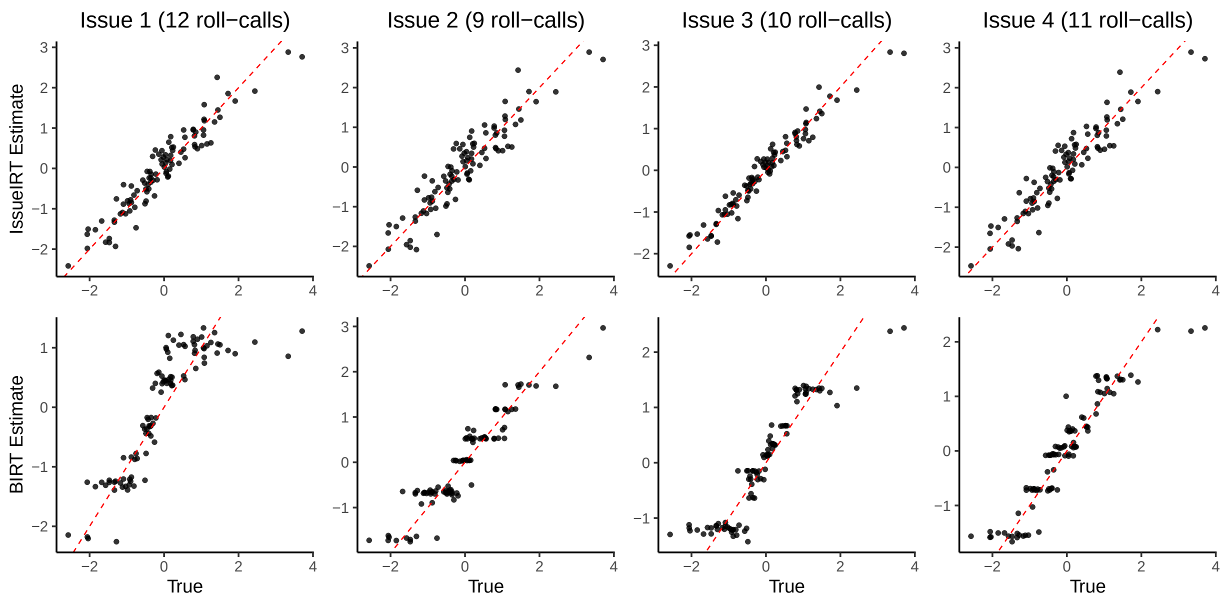

Figure 19: Estimation of issue-specific ideal points for issue A (issues 1 to 4). The results demonstrate that the issue 1 to 4 specific ideal points estimated with our proposed method (top) align well with the true issue A specific ideal points, compared to the subsetting approach (bottom).

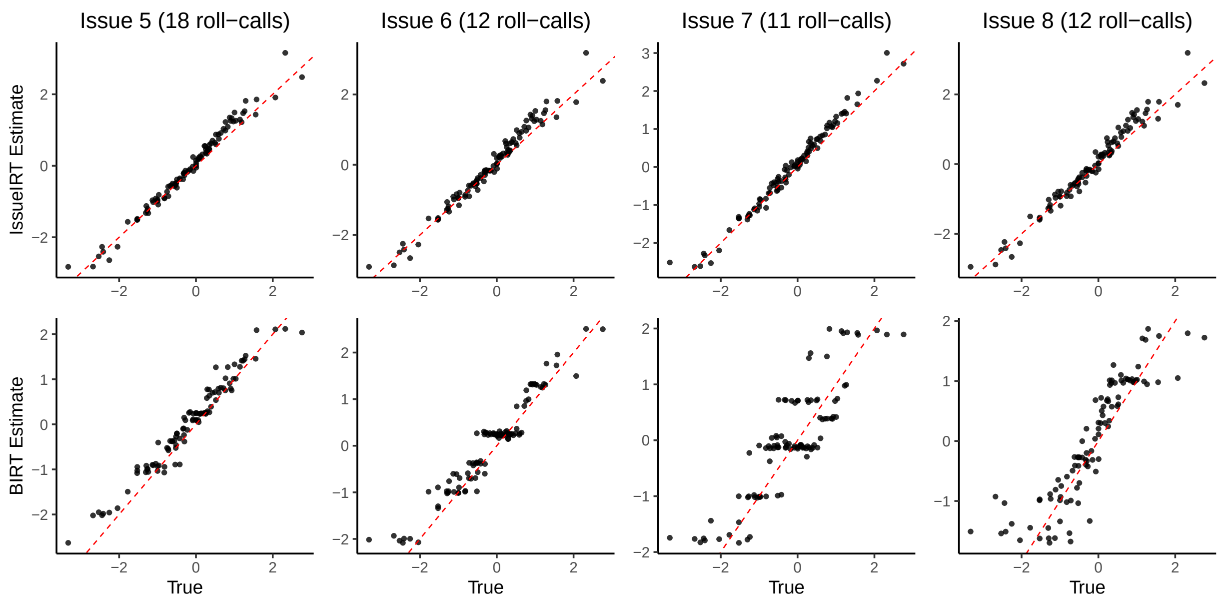

Figure 20: Estimation of issue-specific ideal points for issue B (issues 5 to 9). The results demonstrate that the issue 5 to 9 specific ideal points estimated with our proposed method (top) align well with the true issue B specific ideal points, compared to the subsetting approach (bottom).

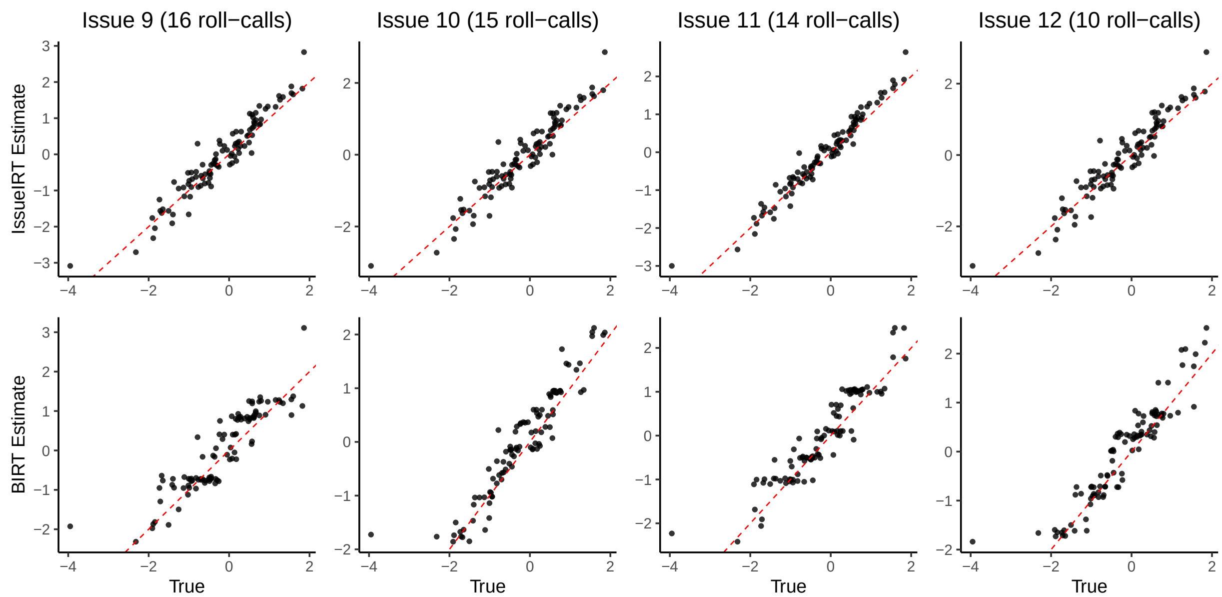

Figure 21: Estimation of issue-specific ideal points for issue C (issues 10 to 12). The results demonstrate that the issue 10 to 12 specific ideal points estimated with our proposed method (top) align well with the true issue C specific ideal points, compared to the subsetting approach (bottom).

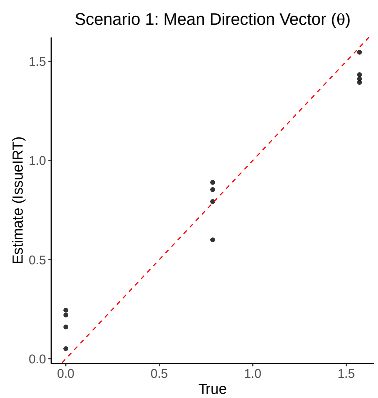

Figure 22: Estimation of issue specific mean direction vector (θ), transformed into angle (Scenario 2). Three legislators were anchored to address rotational invariance for ease of comparison.

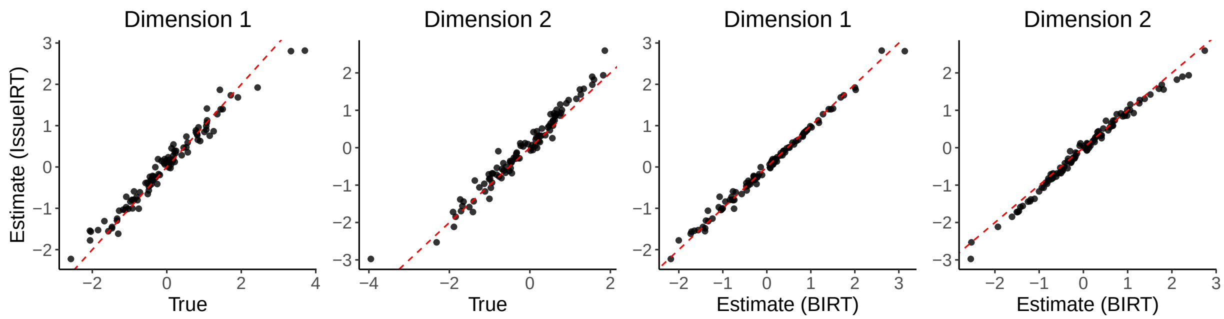

Figure 23: Estimation of multidimensional ideal points (Scenario 2). Three legislators were anchored to address rotational invariance for ease of comparison.

Chain	Warmup (mins)	Sampling (mins)
1	12.24	10.32
2	12.19	7.22

Table 6: Computation time with 2 chains, 1,000 warmup, and 2,000 samples (Scenario 2).

Parameter	Min of $\hat{R}$	25% of $\hat{R}$	Median of $\hat{R}$	75% of $\hat{R}$	Max of $\hat{R}$	Mean of $\hat{R}$
x_{i1}	1	1	1	1	1.01	1
x_{i2}	1	1	1	1	1.01	1
θ_z	1	1	1	1	1	1
u_j	1	1	1	1	1	1

Table 7: Summary of convergence diagnostics ($\hat{R}$) for the simulation study (Scenario 2).

Parameter	Min of ESS	25% of ESS	Median of ESS	75% of ESS	Max of ESS	Mean of ESS
x_{i1}	1649	1904	1960	2014	2128	1948
x_{i2}	1555	1862	1995	2076	2229	1966
θ_z	1824	1970	2016	2085	2115	2011
u_j	1585	1957	2042	2114	2315	2031

Table 8: Summary of effective sample size (ESS) for the simulation study (Scenario 2).

E Additional Results in Application Studies

E.1 The Rise of Populism and Sectional Division in the 1890s

Figure 24 visualizes the monetary-specific ideal points during the 52nd to 54th H.R. using the `IssueIRT` model, demonstrating that the division was sectional rather than partisan. This division is not fully captured by the subsetting approach, as shown in Figure 25. Here, in the top figures, the division between the distribution of the Northeast and the South is not as clear as with the proposed method shown in Figure 6.

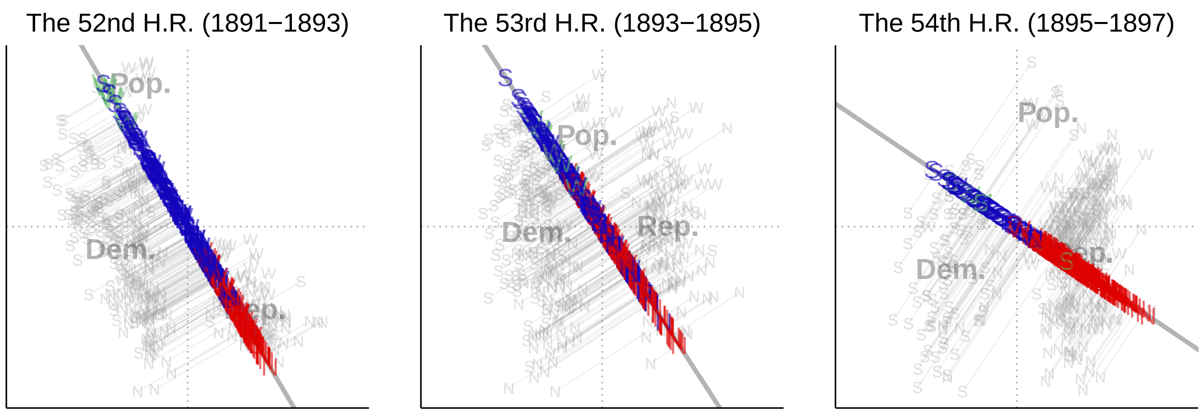

Figure 24: Monetary specific ideal points.

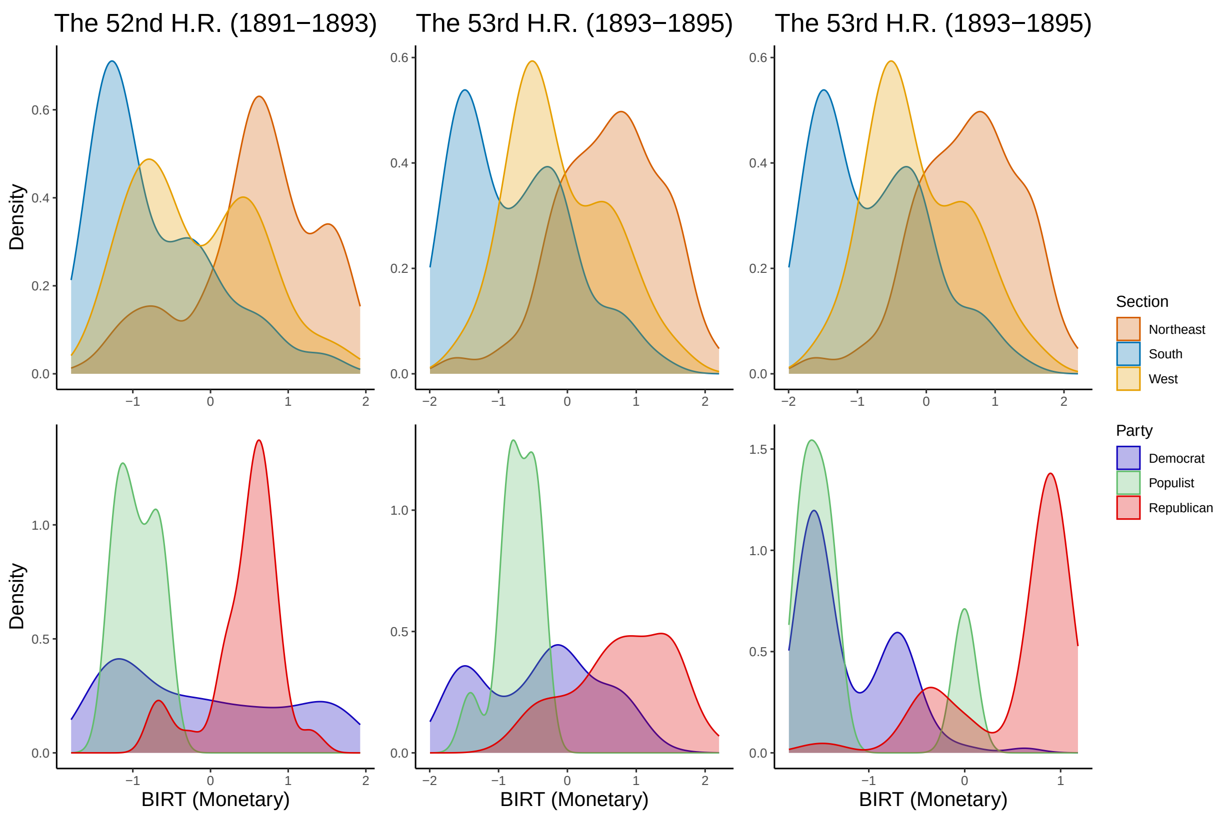

Figure 25: Sectional and partisan distribution of monetary policy specific ideal points using `BIRT` with subsets for each of the 52nd, 53rd, and 54th US H.R. (left, middle, and right figures, respectively).

E.2 Contemporary Congress and Polarization

In this subsection, we consider two measurements of polarization: (1) cosine similarity between the partisan axis and issue-specific axes and (2) the distance between issue-specific party means/-medians. See Supplementary Materials for more details including summary of posterior mean and quantile for each metrics.

E.2.1 Measurement 1: Cosine Similarity

The issue area of "Congress," includes measures concerning members of Congress, general congressional oversight, congressional agencies/committees/operations, legislative procedures, and the U.S. Capitol. Naturally, the legislators' alignment on the "Congress" issue represents the partisan alignment. This implies that by computing the cosine similarity between the direction of "Congress" issue area and that of issue z in each Congress, we can measure the degree of partisan division over issue z during that session ($|\cos(\boldsymbol{\theta}_{\text{congress}}, \boldsymbol{\theta}_z)|$). Note that this resonates with the definition of polarization as "separation of politics into liberal and conservative camps (McCarty, Poole and Rosenthal, 2006, p.3)."

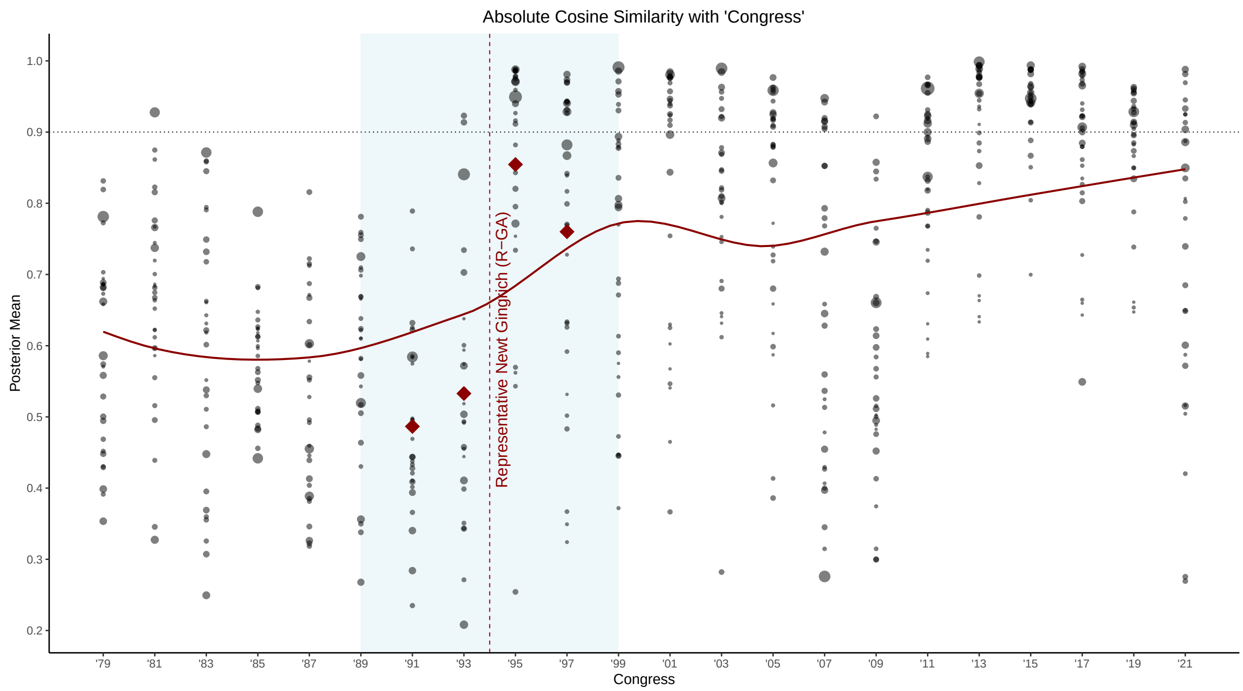

Figure 26: Absolute cosine similarity between "Congress" issue and other issue axes ($|\cos(\boldsymbol{\theta}_{\text{congress}}, \boldsymbol{\theta}_z)|$) across the 96th to 117th US H.R. Each point represents an issue area, where the x-axis is the Congress year and the y-axis is the absolute cosine similarity based on the posterior mean of the direction of issue axes. Values close to 0 represent dissimilarity with partisan division, while 1 represents similarity with it. The diamond points represent the median across issue areas for each Congress.

The absolute cosine similarity between the partisan axis ("Congress" axis) and different issue-specific axes from the 96th to the 117th Congress is shown in Figure 26. Here, I present a LOESS curve (red curve) as a smoothed line to illustrate the general trend across time and issue areas. A few comments can be made. Firstly, we observe an increase over time in the number of issues with estimates exceeding the arbitrary threshold of 0.9 degrees of similarity, indicating that polarization across issue areas has intensified. Secondly, the location of the mean of absolute cosine similarity for each Congress (diamond points) shows a sharp increase after the midterm election of 1994. Lastly, it is noteworthy that both trends – increase in the number of issues with absolute cosine similarity over the arbitrary line and the location of the median of absolute cosine similarity – were initiated during the 104th Congress, the period when Representative Newt Gingrich (R-GA) ascended to power within the Republican Party with his confrontational style and eventually assumed the Speakership.

E.2.2 Measurement 2: Difference in Party Mean/Median

Figure 27 shows the results using the absolute difference in party median as a measurement of polarization. Similarly, Figure 28 use the difference in party mean, but apply a different standardization technique that is robust to outliers: subtracting the median and dividing by the interquartile range. The substantive results are consistent: polarization has increased over time in all issue areas.

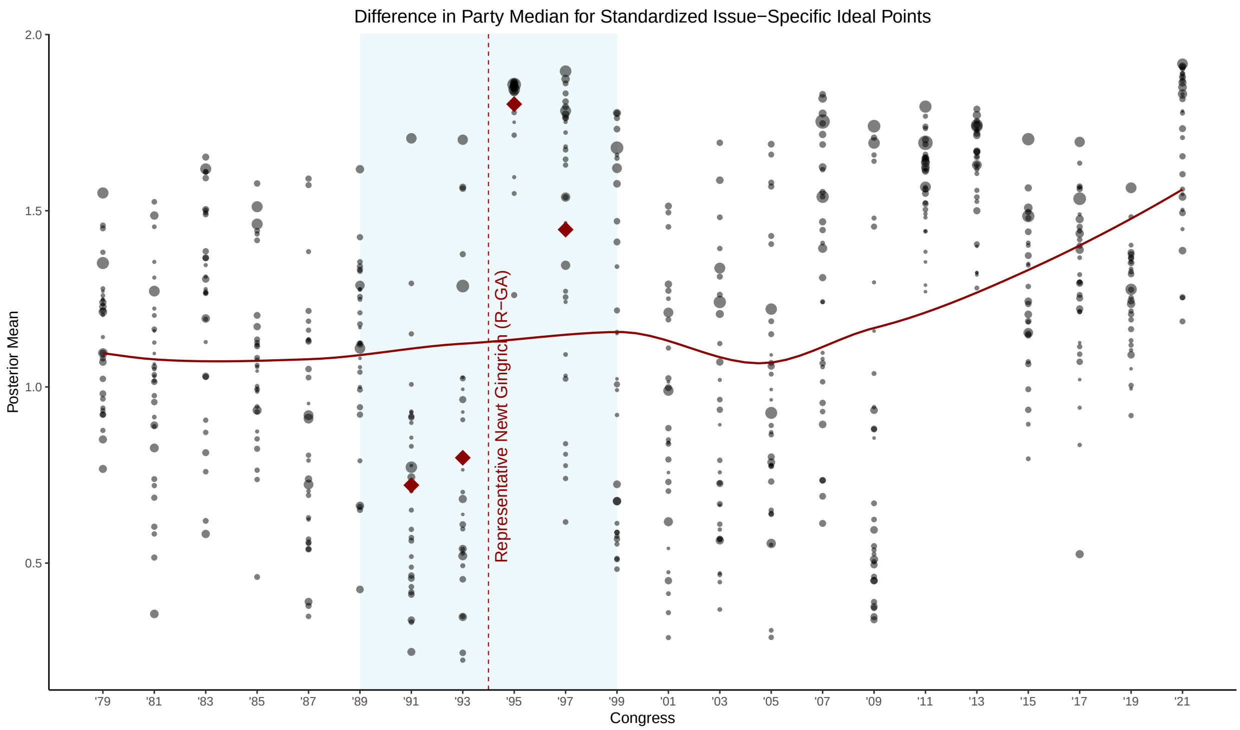

Figure 27: Difference in party median of standardized issue-specific ideal points

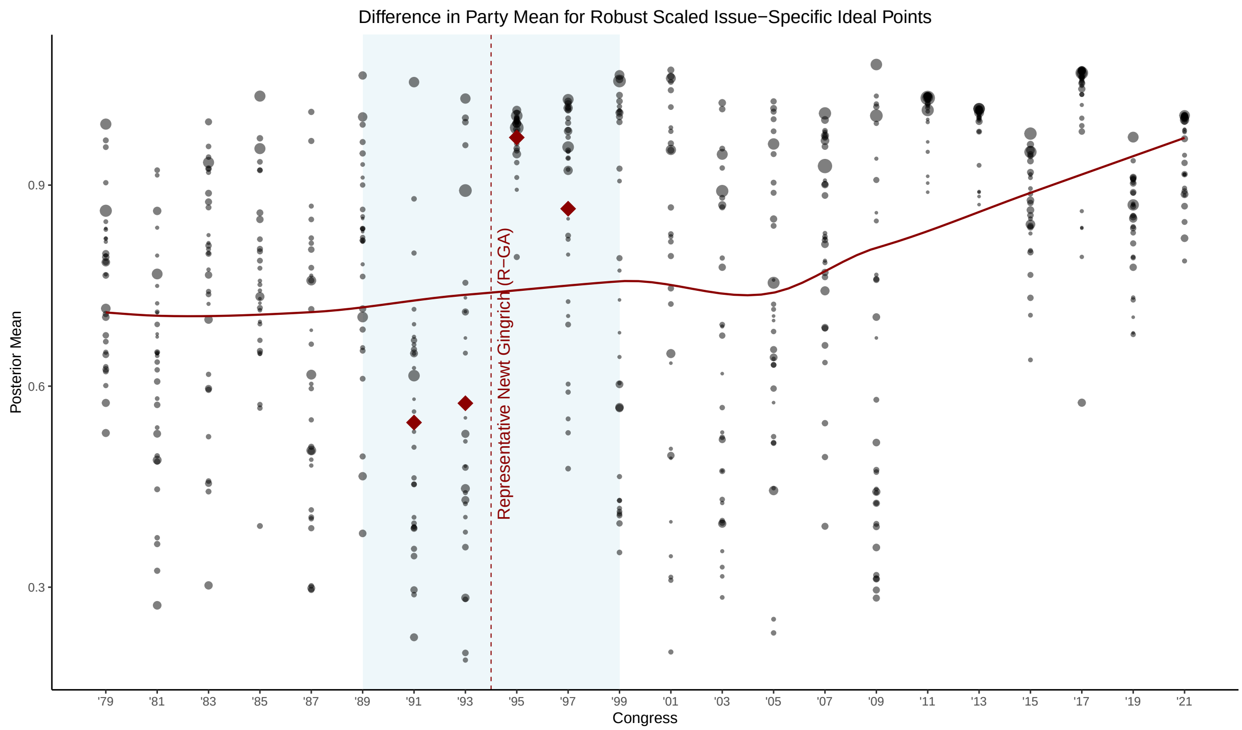

Figure 28: Difference in party mean of standardized issue-specific ideal points using robust scaler.

E.2.3 Dynamic Analysis

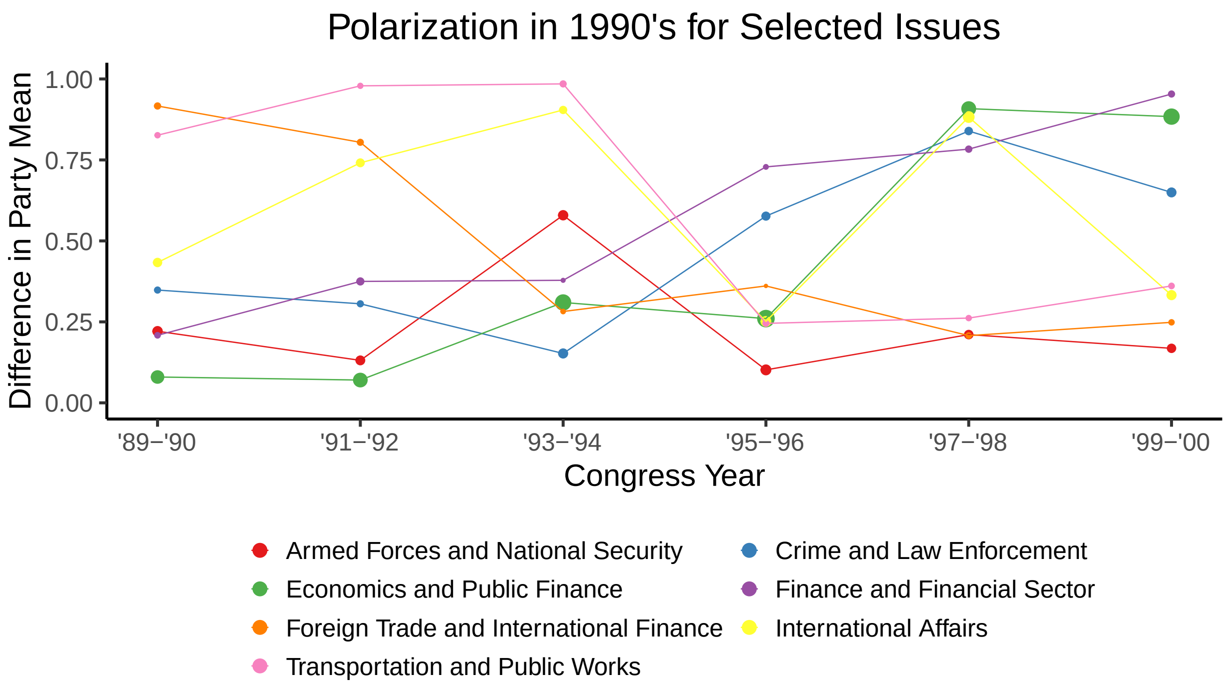

Figure 29: Trajectory of polarization levels during the 1990s. Each line represents the polarization level, measured as the difference in party means, for each issue area over time. The size of the dots is proportional to the number of roll calls.

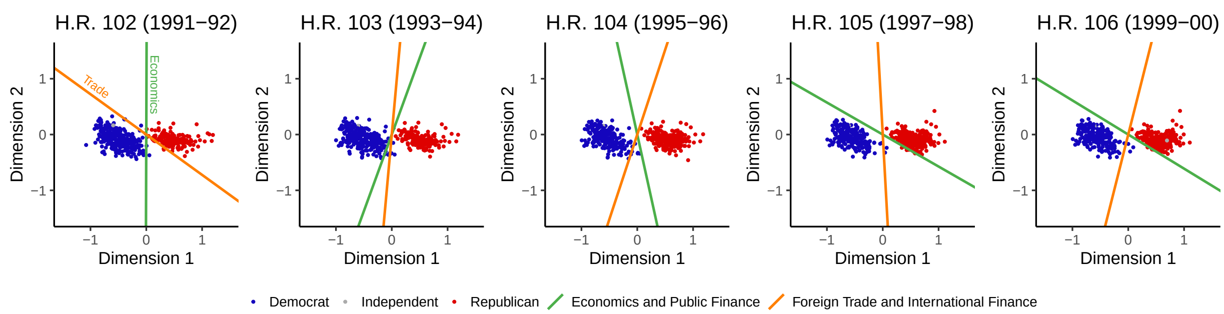

Figure 30: Comparison between public finance-specific (green) and foreign trade-specific axes (orange) in the 1990s. Each dot represents the ideal points of representatives, with color indicating party affiliation (blue for Democrats; red for Republicans).